European Journal of Geography

The publication of the European Journal of Geography (EJG) is based on the European Association of Geographers' goal to make European Geography a worldwide reference and standard. Thus, the scope of the EJG is to publish original and innovative papers that will substantially improve, in a theoretical, conceptual, or empirical way the quality of research, learning, teaching, and applying geography, as well as in promoting the significance of geography as a discipline. Submissions are encouraged to have a European dimension. The European Journal of Geography is a peer-reviewed open access journal and is published quarterly.

Received: 09/04/2024

Revised: 17/06/2024

Accepted: 01/07/2024

Published: 16/08/2024

Academic Editor:
Dr. Alexandros Bartzokas-Tsiompras

DOI: 10.48088/ejg.t.lag.15.3.154.176

ISSN: 1792-1341

Research Article

Comparison and theoretical conceptualization analysis of statistical methods used to develop heat vulnerability indices in urban areas

Thomas Lagelouze [1,2] ✉, Julia Hidalgo [1], Mitia Aranda [1] & Guillaume Dumas [3]

[1] Laboratoire Interdisciplinaire Solidarités Sociétés Territoires (LISST), Université de Toulouse, CNRS, UT2J, 5 Allée Antonio Machado, 31058, Toulouse, France
[2] Institut des Géosciences de l'Environnement (IGE), Université Grenoble Alpes, CNRS, INRAE , IRD, Grenoble-INP, UGA, CS 40700, 38058 Grenoble Cedex 9, France
[3] Toulouse Métropole, Service Observatoire Environnemental, Climat et Transition Écologique, Direction Générale aux Transitions, 6 rue René-Leduc, 31505, Toulouse, France

✉ Correspondence: thomas.lagelouze@univ-grenoble-alpes.fr

Abstract: In view of the impact of extreme temperatures on physical and psychological health, particularly in urban areas, several studies have focused on assessing social vulnerability using quantitative indexing approaches with the aim of creating a heat vulnerability index (HVI). In this context, this study employs three statistical methodologies frequently used to construct HVIs on the territory of the Toulouse Métropole, France, at the census block (IRIS) scale to assess the efficiency of this type of approach for evaluating social vulnerability in urban environments considering the current theoretical conceptualization. The three HVIs show the same general trends, with a spatial configuration in which high levels of vulnerability are concentrated in the downtown and suburbs of the Toulouse municipality. Vulnerability gradually decreases away from the urban core, becoming moderate in the inner suburbs and low on the outskirts. However, a spatial analysis of the clusters reveals variability in the boundaries of the vulnerability hotspots. Value class matching indicates that a significant number of census blocks are classified differently according to the method considered. These results raise questions concerning the ability of HVIs to provide reliable vulnerability assessments, given their geostatistical and conceptual limitations. Indexing approaches therefore appear to contradict current theoretical conceptualizations promoting the concept of vulnerability as being complex and multifactorial.

Keywords: heat vulnerability; statistical index; spatial analysis; results comparison; urban heat island; Toulouse Métropole

Highlights:

- Heat vulnerability indices (HVIs) using three common methodologies are developed.
- Numerous census blocks are categorized differently based on the specific HVI used.
- Alternative approaches for future vulnerability assessments need to be explored.

1. Introduction

The global mean annual temperature was 1.1°C higher between 2011 and 2020 than in the pre-industrial era (IPCC, 2021). This warming has been accompanied by more intense, longer, and more frequent heat waves (Meehl & Tebaldi, 2004), which can sometimes occur earlier or later in the year than normal. Cities have drawn particular scrutiny because of the urban heat island (UHI) phenomenon, which exacerbates temperatures compared with surrounding rural areas (Oke, 1973, 1978), further exposing urban populations (Laaidi et al., 2012), especially during heat-wave episodes (D. Li & Bou-Zeid, 2013).

Heat exposure poses a threat to human health, with heat stress increasing mortality and morbidity (World Meteorological Organization, 2021). In Europe, 93% of deaths linked to natural disasters between 1970 and 2019 were attributed to extreme temperatures. Excluding the European portion of Russia, France had the highest number of heat wave–related deaths in 2003, 2006, and 2015. For example, the 2003 heat wave resulted in over 70,000 deaths in Europe (Robine et al., 2008), with approximately 14,000 deaths due to dehydration, heat stroke, and hyperthermia in France alone between August 1 and 20 (Inserm, 2004). The summer of 2022 was the hottest on record in Europe (Climate Copernicus, 2023), with approximately 62,000 heat-related deaths (Ballester et al., 2023), hitting Italy (~18,000), Spain (~11,000), and Germany (~8,000) the hardest.

The impact of heat varies both socially and spatially as a result of differences in individual physiological, psychological, and socio-economic factors (IPCC, 2023). This introduces the concept of vulnerability to heat: a multidimensional concept (Reghezza-Zitt, 2023) "of causes, outcomes, and pathways" (Karanja & Kiage, 2021, p. 6) that attempts to account for inequalities in the impact of heat on individuals.

The notion of vulnerability to natural hazards has traditionally been linked to that of risk, i.e., the potential for damage when a hazard occurs (Theys & Fabiani, 1987). Geographers in the late 1990s laid the groundwork for its measurement (Blaikie et al., 1994; S. Cutter, 1996; d'Ercole, 1998; Theys & Fabiani, 1987), introducing a social approach to vulnerability, departing from the traditional "hazard-centric" approach. They demonstrated that the "vulnerable" possess certain initial characteristics and resources that make them active in the context of a hazard event (Becerra, 2012); these helps explain the heterogeneity of damage received. Environmental vulnerability has now evolved into a multidisciplinary research domain (Quenault, 2015) used to characterize vulnerability to various environmental hazards such as landslides, avalanches, floods, or heat waves.

Subsequently, because of the above-mentioned health impacts, vulnerability to heat in urban areas is taking a prominent place in the landscape of general vulnerability studies. Although the general definition of vulnerability suffers from polysemy (Becerra, 2012; Quenault, 2015), the scientific literature on heat vulnerability is mostly based on the interconnected parameters of exposure, sensitivity, and adaptive capacity. This conceptual interpretation, relayed and supported by the IPCC (2021), has been defined by Molina et al. (2023) as follows.

- Exposure can be defined as the different ways in which individuals in the same territory are not homogeneously exposed to a climatic event. It simultaneously reflects the societal spatial organization and the spatialization of the hazard in question.
- Sensitivity refers to individuals' reactions to the occurrence of a climatic hazard, inherent to multiple complex processes including physiological, psychological, or socio-economic processes.
- Adaptive capacity represents the ability to mitigate the harmful effects of a disturbance while reducing the impact of the damage suffered.

To assess these parameters, qualitative approaches, primarily from the social sciences, have been utilized; however, there is a shift toward quantitative evaluations in the geosciences. For example, in their literature review, F. Li et al. (2022) demonstrated a quadrupling of quantitative studies between 2006 and 2020. The most popular quantitative models use indexing approaches (F. Li et al., 2022) that result in mapped composite indices (S. L. Cutter et al., 2003), commonly referred to as heat vulnerability indices (HVIs). These indices are designed to condense numerous variables covering various dimensions of vulnerability into a single dimension (Tuccillo & Spielman, 2022) indicative of the overall vulnerability to heat. HVIs offer the advantage of providing a score that summarizes complex phenomena (Wolf et al., 2015), simplifying comprehension of the result and facilitating discussions for adaptation and mitigation strategy development. Consequently, HVIs have become widely used among local authorities as a practical decision-making tool to identify priority neighborhoods requiring territorial climate policy interventions.

While most studies agree on the choice of an index to express vulnerability, the means of constructing such an index differ in many respects.

- First, regarding the input data, typically health, socio-economic, environmental, territorial, and demographic-physiological data are utilized depending on their availability (F. Li et al., 2022; Soomar & Soomar, 2023), covering social, climatic, and spatial aspects for a comprehensive urban heat vulnerability evaluation. The incorporation of these aspects has evolved over time: some studies have focused solely on damage or potential exposure, neglecting social explanatory variables crucial to analyzing societal dynamics (Dousset et al., 2011; Lemonsu et al., 2015), while others have omitted climate variables and failed to integrate social dimensions with physical processes amplifying heat stress in urban settings (Alonso & Renard, 2020; Benmarhnia et al., 2017; Huang et al., 2011; Naughton et al., 2002; Semenza et al., 1996). Additionally, some vulnerability results have lacked spatialization, hindering the identification of socio-spatial inequalities within cities (Huang et al., 2011; Naughton et al., 2002; Semenza et al., 1996). Recent studies, particularly in France (Alonso & Renard, 2020; Forceville et al., 2024; Kastendeuch et al., 2023; Qureshi & Rachid, 2022; Técher et al., 2023), encompass all three aspects. This trend is primarily attributable to advancements in Geographic Information Systems, facilitating data acquisition through remote sensing at finer scales (Wolf et al., 2013), along with new visualization and calculation methods (Zhang et al., 2018). Furthermore, the progressive shift toward a social approach within the vulnerability concept (Bacerra, 2012) has contributed to this evolution. However, while data accessibility has improved, no consensus has yet been reached on the choice of the specific data to be used, or on their spatial and temporal scales, which vary from one study to another (Karanja & Kiage, 2022).
- Second, regarding the statistical methodologies used to construct HVIs, existing literature offers numerous methods. Among the most common are simple additive or multiplicative clustering methods, which aggregate variables based on the vulnerability theoretical conceptualization and principal component analysis. Vulnerability analysis methods based on field surveys and various clustering methods are also employed (de Sherbinin et al., 2019; F. Li et al., 2022). These methods involve data transformation processes to aggregate variables, utilizing weights derived from statistics or expert judgment/questionnaire surveys, as required by the analytic hierarchy process for example. Currently, there is a trend toward equal weighting in the absence of a theoretical basis for doing otherwise (Karanja & Kiage, 2021). In most cases, HVIs are not subjected to validation processes because of challenges in accessing epidemiological data or the workload involved in qualitative validations (Karanja & Kiage, 2021; F. Li et al., 2022).

Because validation processes are still not widespread, some studies call for caution when interpreting HVIs, especially when they are based on a single measurement (Guo et al., 2019), because the results obtained are sensitive to the effects of the methods used (Guo et al., 2019; Liu et al., 2020; Zhu et al., 2014). However, although these observations have been made, recent assessments of heat vulnerability are still frequently based on a single method. In the rare cases in which several methods are used, this limitation is generally not addressed, either out of convenience or habit (Karanja & Kiage, 2021).

Given these premises, this study is divided into two main stages. First, it confirms and reaffirms the conclusions drawn by the aforementioned studies by demonstrating the spatial and statistical variability of vulnerability scores depending on the method employed for the same set of input data. Second, the limits of HVI interpretation are put into perspective by methodologically and theoretically analyzing whether the assessments made by indexing approaches—today used and exploited by many public authorities to plan their adaptation policies—are sufficiently robust and complete to capture vulnerability as it is conceptualized today. To ensure a robust comparison, three methodologies commonly encountered in the scientific literature (F. Li et al., 2022), one of which was identified and tested in a previous study (Lagelouze, 2022), are applied to the Toulouse Métropole, France. Given the demonstrated impact of weightings on HVIs (Karanja & Kiage, 2022), equal weighting is applied to mitigate potential complexities and distortions of the results.

Accordingly, this study is divided as follows: the chosen theoretical concept, study area, data, and methods are discussed in Section 2; the results are presented in Section 3; and the final section is devoted to the discussion and conclusions.

https://doi.org/10.48088/ejg.t.lag.15.3.154.176

2. Data and methods

2.1. Framing the concept of heat vulnerability to urban climate specificities

The concept of vulnerability can be understood as a system of socio-spatial interactions in which the hazard has repercussions. To better illustrate and explain this, this study builds on previous work by risk geographer Patrick Pigeon, updating it with recent semantic advances, enriching it, and focusing it on the domain of heat vulnerability in urban environments.

According to Pigeon (2002), the hazard is influenced by the global environmental context of the study area (the "legacy"), situated in the natural environment, which predetermines its type, occurrence, and intensity. It is then assimilated, modified, and reflected by and within the anthropic environment, where it can be exacerbated by various physical processes (e.g., UHIs), potentially causing social damage depending on the vulnerability system (Figure 1). This system can be understood as the arrangement of "[pre-existing (Karanja & Kiage, 2022)] settlement factors" (Pigeon, 2002) inherent to material, socio-economic and demographic, physiological and psychological, institutional, or cultural criteria, specific to each individual, which leads to an unequal reception of the impact of the hazard. Therefore, the variety of vulnerability criteria makes it both possible and necessary to catalog them to better assess them (Pigeon, 2002). In this regard, settlement factors can be categorized into the three key previously defined parameters: exposure, or the spatial organization of the population; sensitivity, or the physiological, psychological, and socio-economic predispositions of the population to experiencing the hazard; and adaptive capacity, or the mitigation and response mechanisms that prevent or reduce the expected effects of the hazard. The responses of the population can have a direct short-term influence on the anthropic environment and its physical processes and/or an indirect medium- to long-term influence on the natural environment. This combination of elements means that vulnerability is a constantly evolving component of a self-sustaining system. Its factors reflect both static and dynamic actions occurring within a given space, making vulnerability a spatio-temporal notion that is deeply geographical.

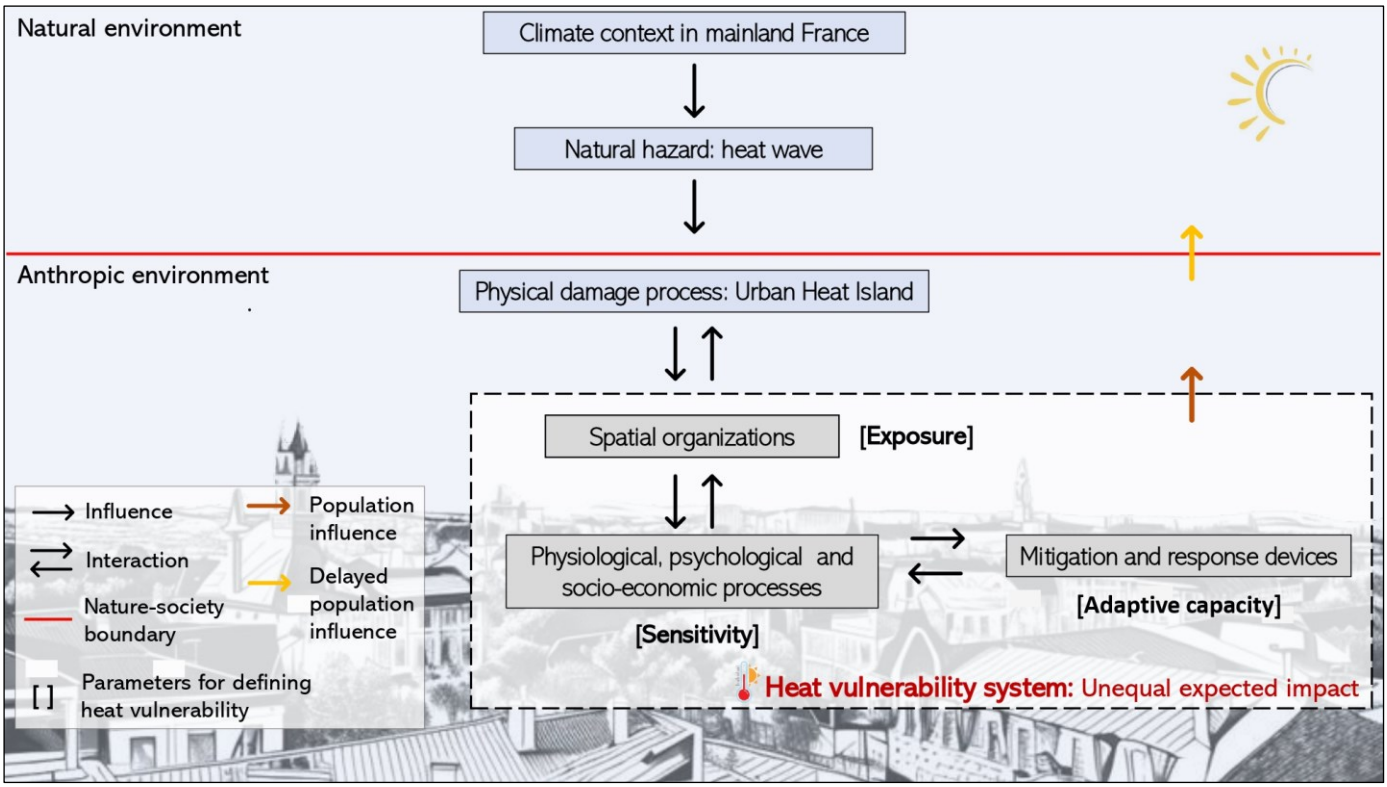

Figure 1. Theoretical conceptualization of the urban heat vulnerability system. Adapted from Pigeon (2002) and Lagelouze (2022).

2.2. Presentation of the study area

The Toulouse Métropole, located in the southwest of France in the Department of Haute-Garonne, is among the 22 largest metropolitan areas in the country, ranking fifth in terms of population with over 800,000 inhabitants in 2020 (Insee, 2024) and spread across 34 municipalities (Figure 2). It is predominantly subjected to a Mediterranean climate according to the Köppen climate classification (*Csa*: warm temperate with hot and dry summers) (Dubreuil, 2022), and daily temperatures exhibit significant variations, ranging from 15°C to 30°C during summer days, with heatwaves reaching up to 40°C (Yin et al., 2022). In 2023, Toulouse experienced new post-August 15 temperature records, indicating a widening summer period with daily highs surpassing 42°C and minimums exceeding 27°C (Lemarque, 2023). From an urban climate perspective, this area is marked by a pronounced heat island effect concentrated in its urban core, as classified by the Suher-Carthy (2021) UHI typology and intensity.

The Toulouse Métropole was chosen as the study area because of its representation of social and urban dynamics prevalent in other French metropolises and globally. Additionally, the urban environment has been spatially discretized into census blocks using "Ilots Regroupés pour l'Information Statistique" (IRIS) units, the smallest demographic census unit in France (Insee, 2024). These units divide municipalities with populations between 5000 and 10,000 inhabitants into several administrative districts and serve as a reference scale for locating, evaluating, and comparing all data in this study. The Toulouse Métropole comprises 251 census blocks.

https://doi.org/10.48088/ejg.t.lag.15.3.154.176

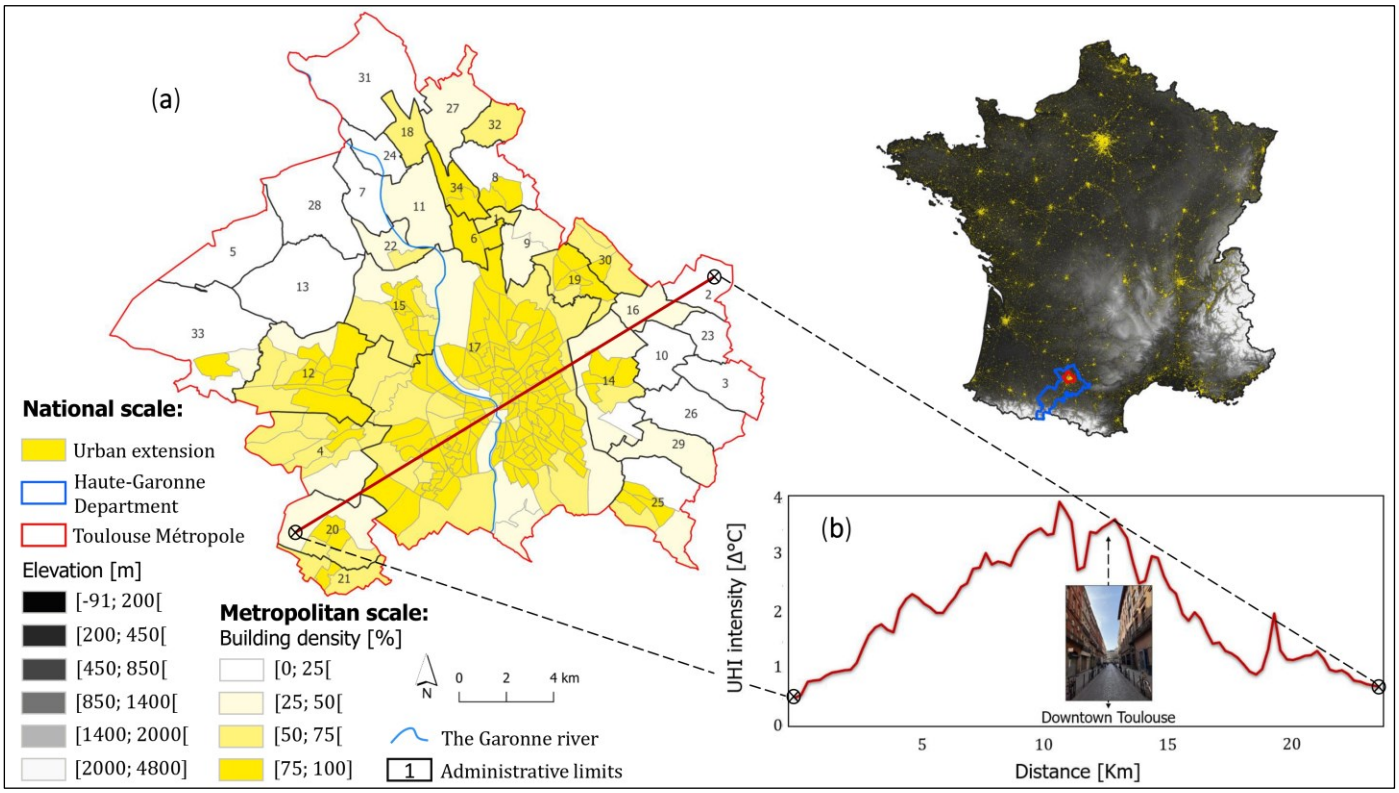

Figure 2. Building density and urban heat island (UHI) intensity in the Toulouse Métropole. (**a**) Location of the Toulouse Métropole in metropolitan France and urban density within census blocks (IRIS units); (**b**) UHI intensity along a transect through the city center. Commune names with their numbers are given in Table A1, and the communes and IRIS units covered by the transect are listed in Table A2. Data Sources: IGN-BD ALTI & TOPO (2022); Centre d'Expertise Scientifique "CES Occupation des sols" (OSO); and MApUCE-UHI dataset.

2.3. Selected data

The set of 24 variables presented in Table 1 corresponds to the data typically utilized in heat vulnerability assessments, as outlined in a literature review by F. Li et al. (2022). These variables were selected to represent the elements influencing and impacting vulnerability during extreme temperature events. Multiple data sources were utilized.

1. Demographic, physiological, and socio-economic variables were provided by the "Institut national de la statistique et des études économiques" (Insee) directly at the IRIS scale.
2. Territorial variables were provided by the "Institut national de l'information géographique" and the "Centre d'Expertise Scientifique - CES Occupation des sols (OSO)" and have been geomatically processed to aggregate them to the spatial reference scale of the study.
3. The climate data were derived from an open-access dataset that characterizes the UHI intensity at a 250-m resolution for 45 French urban areas, as defined in Suher-Carthy et al. (2023).

The demographic variable category (*pd*) assumes that higher population densities correlate with a higher probability of vulnerable individuals (Inostroza et al., 2016). The second category pertains to the physiological health status of the population. Children (*p5*) and the elderly (*p65* and *ret*) are considered more sensitive to heat from an epidemiological perspective. Their bodies have greater difficulty with thermoregulation, which can lead to serious health consequences such as cardiac arrhythmia (Ebi, Capon, et al., 2021; Xu et al., 2014). Female populations (*wo*) are also affected as a result of hormonal cycles (Benmarhnia et al., 2015), as are outdoor worker populations (*pow*) because of increased heat exposure during the day (Ebi, Vanos, et al., 2021).

The socio-economic category has the largest number of variables in this study, as in general in heat vulnerability assessment studies (F. Li et al., 2022). One part of these variables pertains to individual economic capacity (*une*, *ina*, *hlm*, *pr*, and *nhm*), including overcrowded housing (*oc*; Wolf et al., 2013), which affects an individual's ability to protect themselves from heat waves by mobilizing economic capital through purchases or services (Thomas et al., 2019). Another part involves the ability to comprehend and educate oneself about heat dangers, with lower educational levels (*sch* and *cep*) and foreign (*for*) or immigrant (*imm*) status potentially hindering these processes (Kastendeuch et al., 2023; Nayak et al., 2018). A third part addresses social isolation and the potential to address heat responses in specific residential settings. Populations living alone (*cnam* and *pva*) face challenges in accessing support networks during extreme events (Bao et al., 2015; F. Li et al., 2022), and renters (*ren*) have less flexibility: during a situation of discomfort, their room for maneuver and ability to make significant modifications to their housing are limited and depend on their landlord, whether private or social (Molina et al., 2023, p. 45). Lastly, part of the territorial data (*tv*, *urb*, and *topo*) serves as UHI proxies (*uhi*), while another (*pr90*) relates to older dwellings, typically less insulated and therefore exposing residents more strongly to heat (Kastendeuch et al., 2023).

Table 1. Variables used to assess vulnerability to heat. Spatialized data can be viewed in Figure A1.

Variable category	Variable	Data abbreviation	Unit	Impact on vulnerability	Post-acquisition processing	Year of census/data	Data source
Demographic	Population density	*pd*	Ha	(+)	GIS	2017	Insee
Physiological	People aged 65 and over	*p65*	Number	(+)	/	2017	Insee
	People aged 5 and under	*p5*	Number	(+)	/	2017	Insee
	Retirees	*ret*	Number	(+)	/	2017	Insee
	Women	*wo*	Number	(+)	/	2017	Insee
	People aged 15 and over doing physical outdoor work (CSP[1] worker and farmer)	*pow*	Number	(+)	Variables aggregation	2017	Insee
Socio-economic	Unemployed persons aged 15 to 64	*une*	Number	(+)	/	2017	Insee
	Inactive people aged 15 to 64	*ina*	Number	(+)	/	2017	Insee
	People living in low-income housing (HLM[2]) as their main residence	*hlm*	Number	(+)	/	2017	Insee
	Poverty rate	*pr*	%	(+)	/	2017	Insee
	Non-household members	*nhm*	Number	(+)	/	2017	Insee
	Primary residences (excluding 1-person studio) over-occupied	*oc*	Number	(+)	/	2017	Insee
	People aged 15 and over not attending school	*sch*	Number	(+)	/	2017	Insee
	People aged 15 and over not attending school, without degree or CEP[3]	*cep*	Number	(+)	/	2017	Insee
	Foreigners	*for*	Number	(+)	/	2017	Insee
	Immigrants	imm	Number	(+)	/	2017	Insee
	CNAM[4] beneficiaries	*cnam*	Number	(-)	/	2020	Insee
	People living alone	*pva*	Number	(+)	/	2017	Insee
	People renting primary residences	*ren*	Number	(+)	/	2017	Insee
Territorial	Principal residences built before 1990	*pr90*	Number	(+)	Variables aggregation	2017	Insee
	Tall vegetation	*tv*	%	(-)	GIS	2022	Centre d'Expertise Scientifique « CES Occupation des sols » (OSO)
	Urban zone	*urb*	%	(+)	GIS	2022	Centre d'Expertise Scientifique « CES Occupation des sols » (OSO)
	Topography	*topo*	m	(-)	GIS	2023	IGN-BD ALTI (25m)
Climatic	UHI intensity	*uhi*	Δ°C	(+)	GIS	2014	UHI Dataset -DOI: 10.5281/zenodo.8009878

[1] Socio-professional categories, French statistical nomenclature used to classify occupations.

[2] Low-rent housing

[3] Professional Development Consulting, free French public service, accessible to employees and self-employed people

[4] National Health Insurance Fund, manages the sickness (sickness, maternity, disability, death) and industrial accident/occupational disease branches of the French Social Security system

2.4. Methodologies

Three methods, belonging to the family of indexing approaches, were chosen and are compared for their common use in developing HVIs (F. Li et al., 2022).

1. Principal component analysis (PCA), the most widely utilized method for reducing variables to an index (Sanders, 1989), is a multivariate statistical technique designed to decrease the dimensionality of a dataset while retaining as much information as possible (Berger, 2022). It transforms interdependent variables into a new set of orthogonal variables, known as principal components or, in this context, vulnerability factors.
2. The hierarchical agglomerative clustering method based on the PCA first component (PCA-HAC), a method proposed by Chavent et al. (2012), employs the ClustOfVar package in R and is specifically dedicated to clustering quantitative and/or qualitative variables. While not previously utilized for constructing HVIs, it falls within the category of already-explored clustering methodologies.
3. Theoretical component (TC), often used in the literature with equal weightings (F. Li et al., 2022), involves constructing an HVI according to the theoretical conceptualization of the vulnerability.

These methods work by grouping the variables presented in the previous section into several distinct entities. To form the groups and the final HVIs, the choice was made to sum the variables among themselves, as is generally done in the scientific literature and in the absence of adequate underlying and existing logical relationships between the constituent elements to justify the use of other arithmetical paths (F. Li et al., 2022). The entire study process is illustrated in Figure 3; the processes used to construct the HVIs and determine their spatial patterns are described in detail in the following subsections.

2.4.1. Preprocessing

In developing an HVI, a preprocessing phase of the variables is essential to ensure their statistical conformity with the subsequent methodologies. First, each variable must contain a consistent amount of information. Therefore, variables with more than 5% missing data and IRIS units containing at least one missing data point were excluded (Figure A2). Subsequently, potential collinearity between pairs of variables is addressed to prevent the aggregation of variables representing similar information, which could lead to an over-representation of certain vulnerability dimensions. Variables with Bravais–Pearson correlation coefficients greater than or equal to 0.8 or less than or equal to −0.8 were removed (OECD et al., 2008). Before calculating the correlation matrix, data with a Shapiro–Wilk test with a *p*-value of less than 0.05 were Gaussian-transformed using the Yeo–Johnson method (Yeo & Johnson, 2000) to optimize the results (Figure 4). Following normalization, variables were centered and reduced using the zero-mean standardization method to facilitate comparisons by generating unitless data with equivalent means and dispersions.

2.4.2. Principal component analysis application

When conducting a PCA, it is advisable to assess whether the variables remain sufficiently redundant to be summarized without being excessively collinear. To analyze the data redundancy, the Kaiser–Mayer–Olkin (KMO) index (Kaiser, 1974) was calculated to measure the "compressibility" of the data. The KMO index compares the raw correlation with the partial correlation for the same variable, disregarding the influence of other relationships in the dataset. An overall index greater than 0.6 characterizes a fairly redundant dataset (OECD et al., 2008). The *topo* (topography) variable exhibited a low individual KMO index (0.44) and was therefore removed because it was likely orthogonal to the other variables in the PCA. Note that, for the subsequent methods, this variable was also excluded to maintain result comparability. The global KMO index was then 0.73. A secondary test of a similar nature was performed using the standardized Cronbach's *alpha* (Cronbach, 1951). A mean correlation was utilized to assess the dataset homogeneity, with the recommended *alpha* threshold being above 0.7 (OECD et al., 2008); in this case, *alpha* was 0.79. Finally, Bartlett's sphericity test (Anastassakos & d'Aubigny, 1984) was conducted, comparing the observed correlation matrix with the identity matrix to validate the hypothesis of non-significant correlation among variables. With all preconditions met, a varimax rotation PCA was run to maximize correlations with the factor axes (Kaiser, 1958).

To determine the number of factors—that is, the dimensions that most effectively summarize the dataset—into which variables can be grouped, the observed (λ_{obs}) and simulated (λ_{sim}) eigenvalues of the PCA dimensions were analyzed. Simulated eigenvalues were obtained by bootstrapping repeatedly for 1000 iterations using the Monte–Carlo approach (Peres-Neto et al., 2005) in which a dataset following a normal distribution $N(0,1)$ of the same dimensions as our dataset was randomly generated. A factor is considered relevant when $\lambda_{obs} > q^{95}(\lambda_{sim})$ (Rakotomalala, 2012); as such, three dimensions were retained for our dataset (Figure 5). Within the three components, each variable was aggregated on the component for which it had the highest factor weight (Table 2). Accordingly, variables with a positive impact on vulnerability were added together, while variables with a negative impact were subtracted (Table 1). Finally, factor aggregation was performed on the raw variables, which were standardized using the min-max method to eliminate the unit effect.

2.4.3. Hierarchical agglomerative classification application

The PCA-HAC method is based on an HAC algorithm embedded in the ClustOfVar package (Chavent et al., 2012). The aim of the PCA-HAC method is to find a partition of a set of p mixed variables x_j sufficiently related to each other to belong to the same cluster, denoted C_k. In other words, the objective is to find a partition $P_k = (C_1, \ldots, C_k)$ that maximizes the homogeneity $H(P_k)$, where $H(P_k) = \sum_{k=1}^{K} H(C_k)$. Initially, each variable constitutes a cluster; the variables with the smallest dissimilarity are then aggregated as follows: $d(C_1, C_2) = H(C_1) + H(C_2) - H(C_1 \cup C_2)$. Here, with only numeric variables, $H(C_k)$ was measured via the Bravais–Pearson correlation between the variables of the cluster and a numeric synthetic variable y_k summarizing the cluster, such that $H(C_k) = \sum_{x_j \in C_k} r^2_{(x_j, y_k)} = \lambda_1^k$. y_k is the first principal component of the PCA of the PCAmixdata package in R (Chavent et al., 2022) applied to the data of the cluster (Saracco et al., 2018): $y_k = arg\ max_{u \in \mathbb{R}^n} \left\{ \sum_{x_j \in C_k} r^2_{(x_j, u)} \right\}$. λ_1^k is then the first eigenvalue of the PCAmixdata PCA applied to the variables belonging to the class C_k.

A bootstrap procedure with 1000 iterations evaluating the stability according to the Rand index (Rand, 1971) of the p partitions to determine the appropriate number of classes was then applied and suggested a total of 6–7 classes (Figure 6). Finally, three clusters were selected because

the PCA applied to each of them returned each time only one eigenvalue greater than 1. The cluster characteristics and composition are presented in Table 3. The general cluster is the result of adding the three clusters, considering the same criteria as in the previous method.

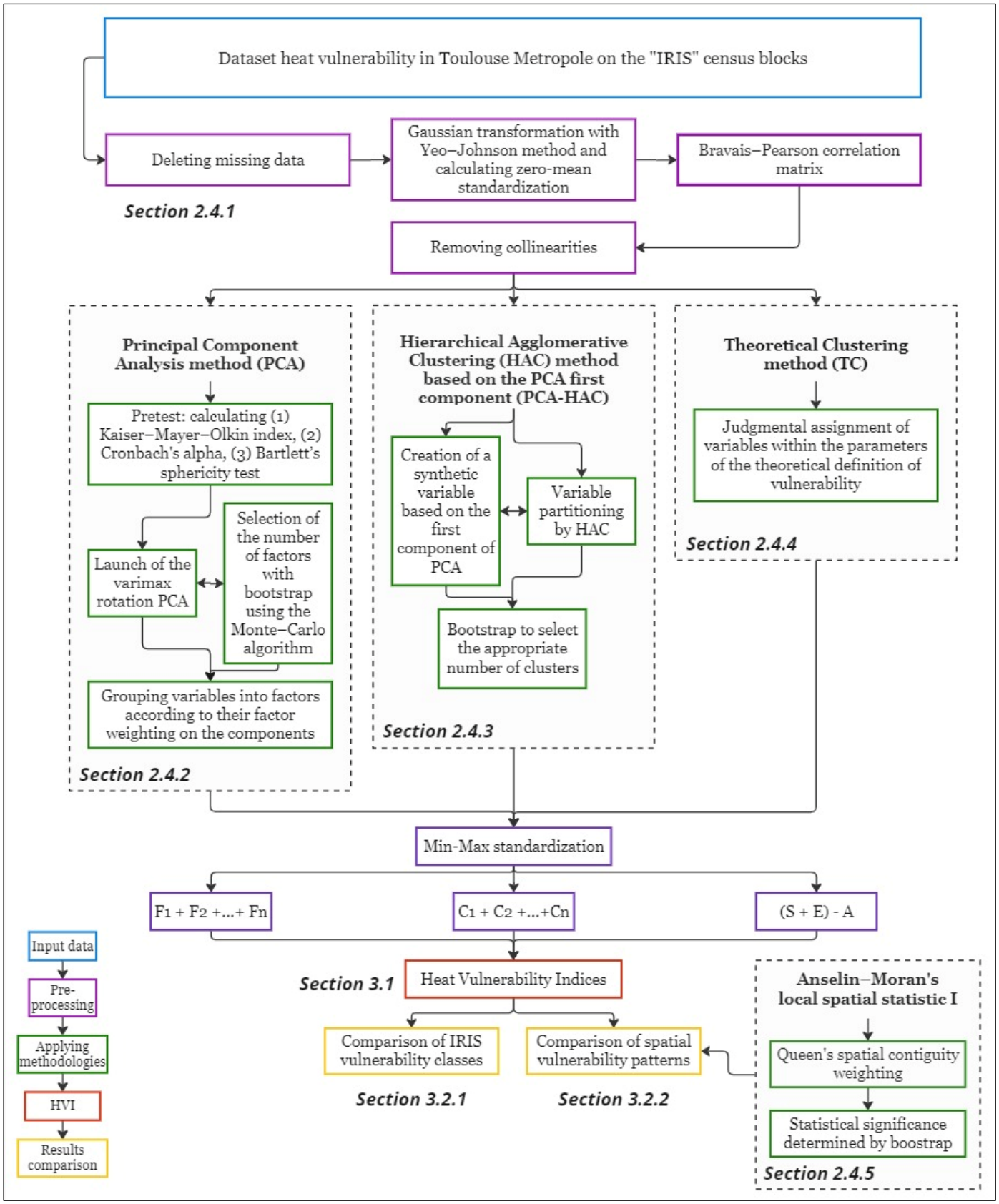

Figure 3. Processes used to create the heat vulnerability indices (HVIs).

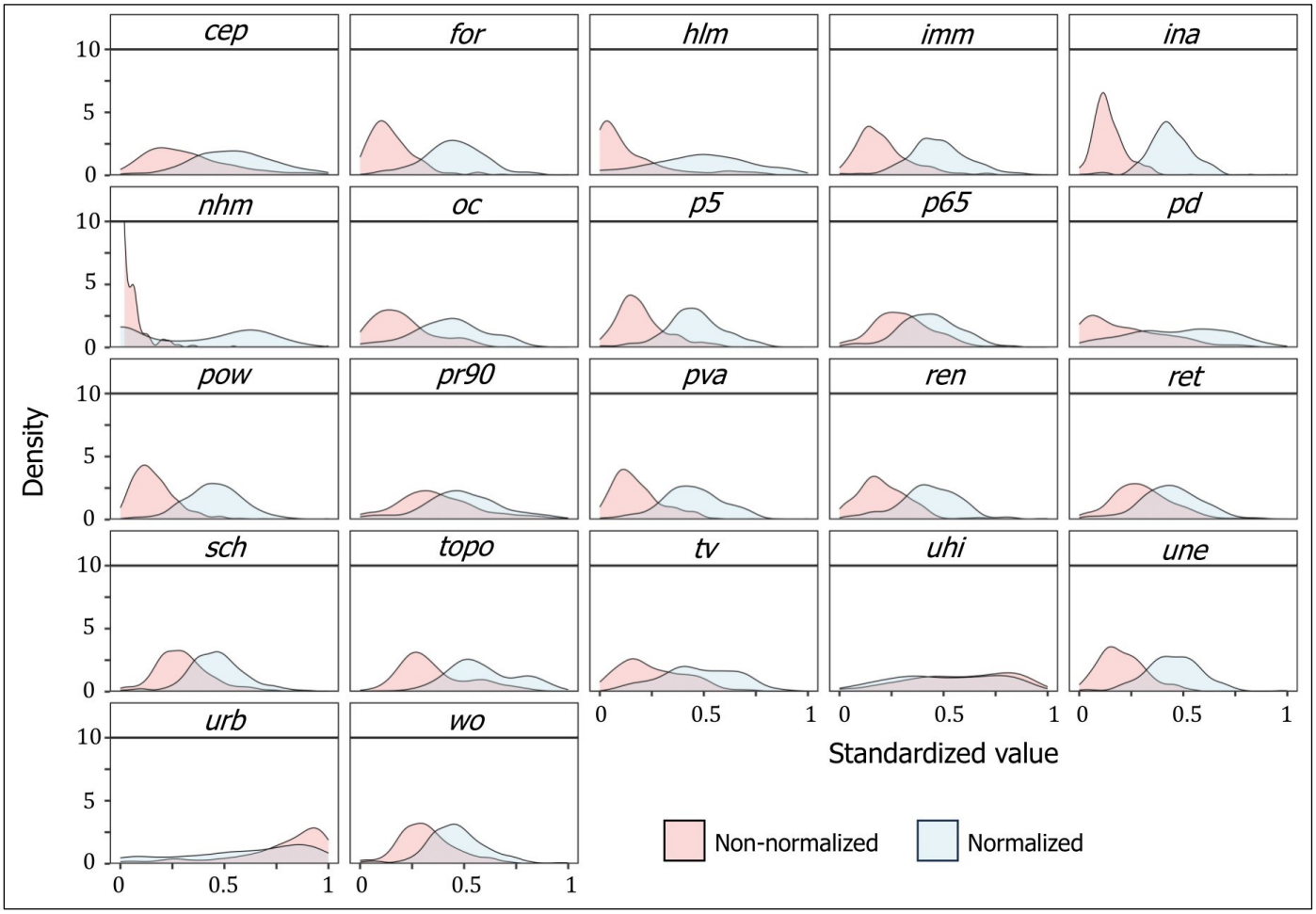

Figure 4. Statistical distribution of the variables before and after the Yeo–Johnson transformation. For variable definitions, see Table 1.

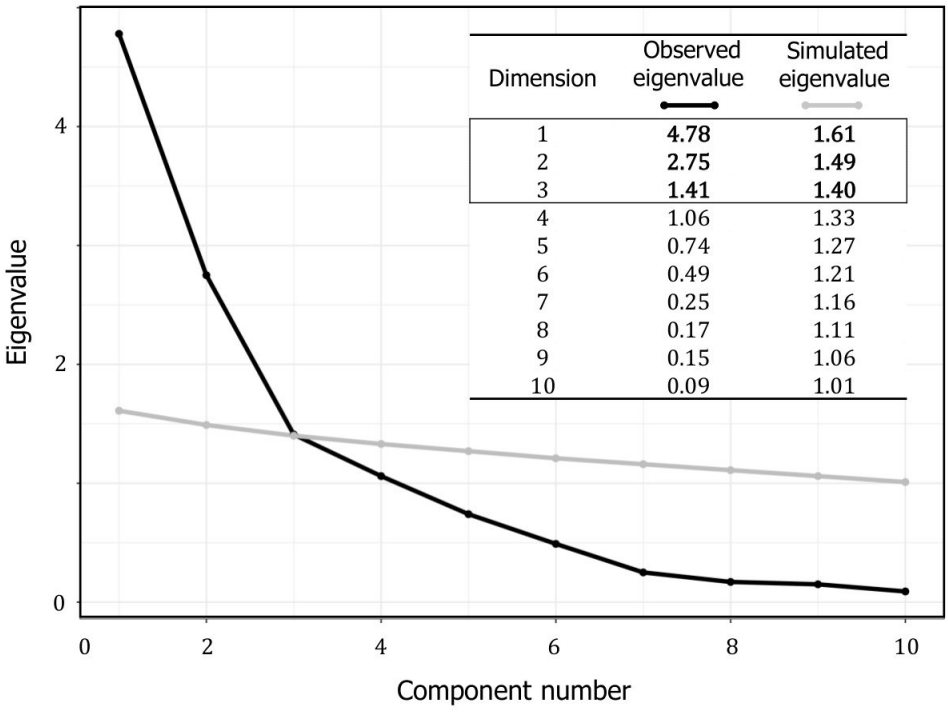

Figure 5. Process for selecting the number of dimensions by comparing the observed and simulated eigenvalues.

https://doi.org/10.48088/ejg.t.lag.15.3.154.176

Table 2. Factor weights obtained on the three selected principal component analysis (PCA) components. The highest factor weight for each variable is highlighted in bold.

Variable	Factor 1	Factor 2	Factor 3
urb	0	0.56	0.64
tv	−0.02	−0.19	−0.98
uhi	−0.02	0.93	0.26
une	0.83	0.26	0.05
sch	0.76	−0.01	0.02
pva	0.37	0.33	0.05
hlm	0.42	0.04	−0.02
pr90	0.12	0.49	0.13
p65	0.28	−0.02	0.04
p5	0.91	−0.09	−0.03
pow	0.91	−0.07	0.01
nhm	0.09	−0.03	−0.11

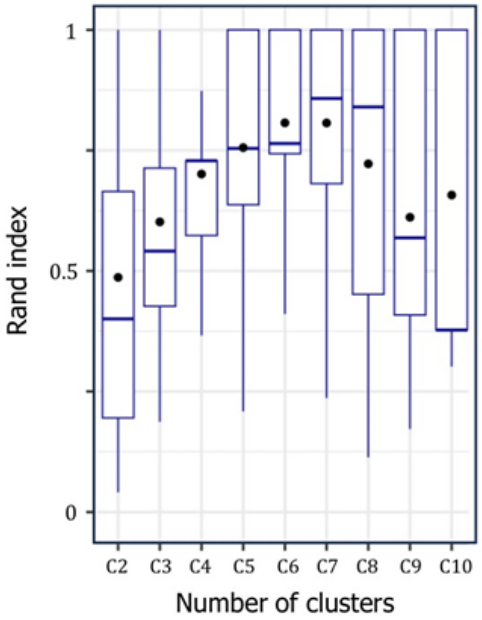

Figure 6. Dispersion of the adjusted Rand index.

Table 3. Assignment of clusters to variables and correlation using the hierarchical agglomerative clustering method based on the PCA first component (PCA-HAC).

Variable	*urb*	*tv*	*uhi*	*une*	*sch*	*pva*	*hlm*	*pr90*	*p65*	*p5*	*pow*	*nhm*
Cluster Number	1	1	1	2	2	3	2	3	3	2	2	3
$r^2_{(x_j,y_k)}$	0.95	0.83	0.83	0.89	0.86	0.85	0.67	0.88	0.67	0.94	0.95	0.37

https://doi.org/10.48088/ejg.t.lag.15.3.154.176

2.4.4. Theoretical clustering application

The TC method assumes that each numerical variable corresponds to one of the three vulnerability parameters: Exposure (E); Sensitivity (S); or Adaptive Capacity (CA), as illustrated in Figure 1 and assigned in Table 4. Consequently, the overall heat vulnerability is calculated as the sum of the exposure and sensitivity, subtracting the adaptive capacity. In this method, variables are standardized to eliminate units and aggregation is performed manually based on a subjective ruling linked to theory.

Table 4. Assignment of variables to the vulnerability parameters: Exposure (E); Sensitivity (S); and Adaptive Capacity (CA) in the theoretical clustering (TC) method.

Variable	**urb**	**tv**	**uhi**	**une**	**sch**	**pva**	**hlm**	**pr90**	**p65**	**p5**	**pow**	**nhm**
Parameter	E	CA	E	S	S	S	S	E	S	S	S	S

2.4.5. Spatial pattern identification of the vulnerability

Spatial patterns of the HVI scores were identified by analyzing the spatial autocorrelation using the Anselin–Moran local spatial statistic I (Anselin, 1995) for each method previously presented and in each IRIS unit. Spatial neighbors were categorized considering Queen's contiguity. The statistic was deemed significant for a *p*-value of less than 5%, obtained after a simulation of 1000 conditional permutations. Four types of clusters can then be identified: (1) High-High clusters, IRIS units with high vulnerability surrounded by other IRIS units with high vulnerability; (2) High-Low clusters, IRIS units with high vulnerability surrounded by IRIS units with low vulnerability; (3) Low-High clusters, IRIS units with low vulnerability surrounded by IRIS units with high vulnerability; and (4) Low-Low clusters, IRIS units with low vulnerability surrounded by other IRIS units with low vulnerability.

3. Results

3.1. Presentation of results

The results obtained for each method are jointly analyzed and spatially examined using three approaches. First, the composition and spatialization of the vulnerability groups are scrutinized using equal-interval discretization to enhance their comparability. Second, the statistical distribution of an HVI is depicted by discretizing it using Jenks' natural threshold method to identify threshold effects indicating potential increases or decreases in the vulnerability. Third, a mapping is proposed based on this discretization, where an HVI close to 1 indicates higher vulnerability levels for an IRIS unit.

3.1.1. PCA results

Three factors were formed during the PCA application, each exhibiting distinct structures (Table 2). Factor 1 groups 7 of the 12 variables retained post-preprocessing. These variables predominantly pertain to the socio-economic and physiological status of the population, focusing on poverty, age, and employment. Conversely, Factor 2 can be construed as a climatic factor, comprising the UHI variable, which carries a higher factorial weight than the territorial variable representing the number of buildings constructed prior to 1990. These variables have similar spatial distributions, with maximum intensities concentrated in the downtown Toulouse area. Factor 3 exhibits continuity with Factor 2, encompassing the territorial variables of the building density and tall vegetation, which are inversely correlated on the same PCA component. The variable *nhm* (non-household members) is also incorporated into this factor, albeit with a low factorial weight on the third dimension, similar to its representation on the first two dimensions. This variable demonstrates a weak receptivity to the PCA methodology, placing it within a dimension without necessarily exhibiting a statistical coherence that explains its relation to the other variables.

The statistical distribution of the HVI depicted in Figure 7(b) reveals a notable proportion of census blocks situated in classes 3 (34%) and 4 (29%), with a marked break at an index value of 0.63, indicating a transition from moderate to high vulnerability. The 24 IRIS units identified as the most vulnerable are categorized in class 5, with an index equal to or greater than 0.78, and are exclusively situated within the municipality of Toulouse. Spatially (Figure 7(c)), these IRIS units are concentrated in the city center and its suburban regions on both the right and left banks of the Garonne (e.g., IRIS *Concorde*); this is attributed to the combined influence of all three factors, primarily Factor 2 (Figure 7(a)). Moreover, the northeastern region of the city is also affected, exemplified by districts such as *Lalande Nord* and *Borderouge Nord*, which exhibit high concentrations of households characterized by unemployment (*une*), individuals working outside the home (*pow*), individuals lacking qualifications (*sch*), and young dependents (*p5*), all of which contribute to Factor 1. Similarly, the *Latécoère* district in the southeast experiences heightened vulnerability because of the significant density of non-household members (*nhm*) associated with Factor 3 (Figure A1). In summary, the metropolitan HVI spatial pattern is concentric, with vulnerability diminishing around the first urban rings around Toulouse, although certain municipalities, such as *Villeneuve-Tolosane* in the extreme southwest with all of its census blocks falling into class 3, represent exceptions.

https://doi.org/10.48088/ejg.t.lag.15.3.154.176

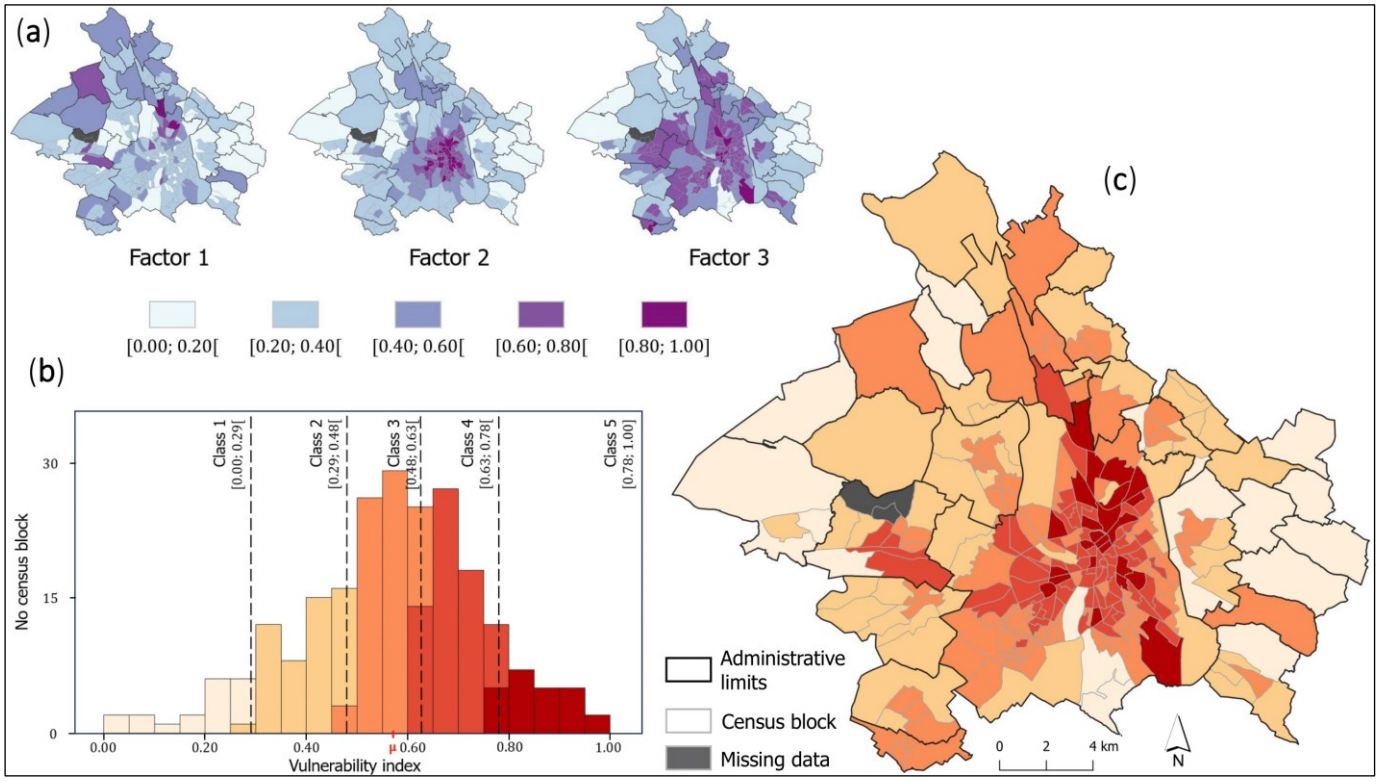

Figure 7. HVI obtained using the principal component analysis (PCA) method on the Toulouse Métropole. (**a**) Spatial distribution of the three vulnerability factors; (**b**) discretization and statistical distribution of the HVI; (**c**) final HVI.

3.1.2. PCA-HAC results

The PCA-HAC method generated three clusters comprising highly correlated variables that are more easily interpretable from a theoretical standpoint (Table 3). Cluster 1 distinctly delineates the climatic dimension, grouping the UHI variable with its primary proxies, the built-up density, and tall vegetation. In contrast, Cluster 2 is geared toward socio-economic capacities, emphasizing social groups with limited financial resources and engaging in physically demanding occupations. Cluster 3 exhibits a more composite nature, portraying a vulnerability profile rather than a distinct category of variables: individuals aged 65 and older (*p65*) in the Toulouse Métropole exhibit a higher likelihood of living alone (*pva*) in older housing (*pr90*).

The HVI exhibits a relatively linear distribution across the Toulouse Métropole IRIS units, with 37% clustered around the mean (0.52) in class 3 (Figure 8(b)), contrasting with 12% and 9% for classes 1 and 5. Notably, breakpoints between high (class 4) and very high (class 5) vulnerability, as well as between very low (class 1) and low (class 2) vulnerability, are situated at index values of 0.73 and 0.32, respectively. Spatially, vulnerabilities are accentuated in downtown Toulouse census blocks (Figure 8(c)) as a result of the climatic factors outlined in Cluster 1, while in northeast and southeast IRIS units, socio-economic structures delineated by Clusters 2 and 3 predominantly contribute to the vulnerability patterns (Figure 8(a)). However, the reduced number of socio-economic-physiological variables in Clusters 2 and 3 highlights specific spatial distributions of the vulnerability that were previously smoothed out by numerous variables. Consequently, the vulnerability indices in class 5 extend beyond the commune of *Toulouse*, encompassing the first urban ring to the west in IRIS units such as *Perget Est* and *Cabirol-Ramassiers* in the commune of *Colomiers*, characterized by populations lacking qualifications (*sch* - Cluster 2) and elderly individuals (*p65* - Cluster 3; Figure A1). Notably, the municipality of *Quint-Fonsegrives* to the east emerges as highly vulnerable in Cluster 3, contrasting with its previous moderate-vulnerability status under the socio-economic Factor 1. Ultimately, despite the various intricacies outlined in this section, the least vulnerable communes remain the most peripheral of the Toulouse Métropole, particularly to the east, with *Beaupuy*, *Mondouzil*, *Pin-Balma*, and *Mons* exhibiting index values less than or equal to 0.20 across all three clusters.

https://doi.org/10.48088/ejg.t.lag.15.3.154.176

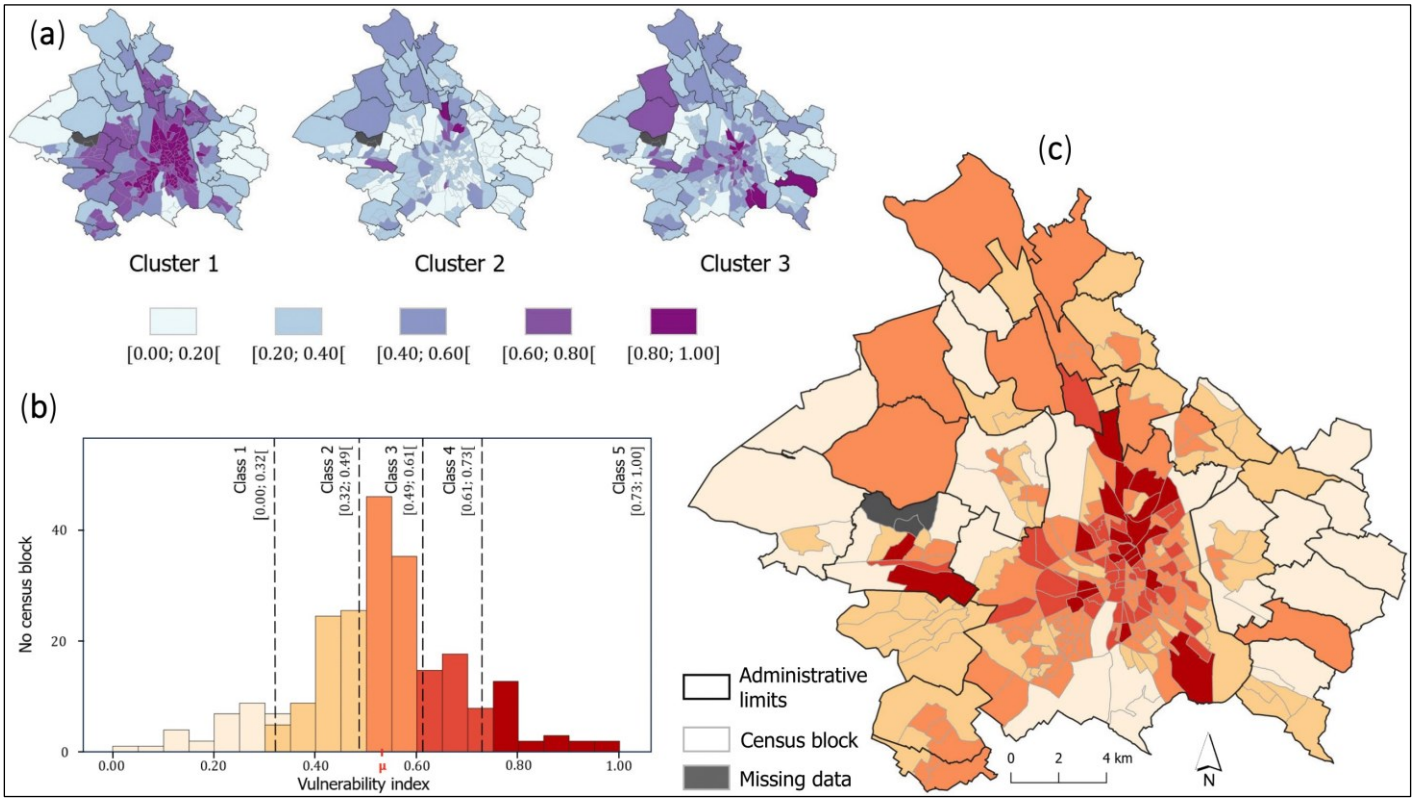

Figure 8. HVI obtained using the hierarchical agglomerative clustering method based on the PCA first component (PCA-HAC) on the Toulouse Métropole. (**a**) Spatial distribution of the three vulnerability factors; (**b**) discretization and statistical distribution of the HVI; (c) final HVI.

3.1.3. TC results

The theoretical conception categorized the 12 variables into three distinct groups (Table 4). Socio-economic and physiological variables were grouped under the Sensitivity parameter, climatic and territorial variables under the Exposure parameter, and tall vegetation under the Adaptation Capacity parameter, highlighting potential cooling solutions. This approach established groups that are coherent in their interpretation but disparate in the number of variables considered. Notably, the Sensitivity group encompasses 8 of the 12 variables, reflecting the initial predominance of socio-economic variables (Table 1). This predominance generates well-represented variables for those with similar distribution patterns, such as *une*, *p5*, and *pow*, unlike variables with a singular pattern such as *p65*. The Exposure group exhibits no significant changes, while the Adaptive Capacity group comprises a single variable. Neighborhoods with high indices in Figure 9(a) correspond to low vulnerability; this is particularly evident in the southern green zones of the commune of *Toulouse* such as *Pouvourville* and *Coteaux de Pech-David*, as well as in the western agricultural communities of *Mondonville* and *Pibrac*.

A total of 40% of the census blocks are in the high-vulnerability class 4, and 13% (or 33 IRIS units) are in the very-high-vulnerability class 5, explaining the slightly higher average of 0.56 (Figure 9(b)). Many IRIS units in downtown Toulouse and the surrounding suburbs shift from class 4 to class 5, such as *Les Violettes* in *Aucamville*. Conversely, *Latécoère* in the southeast of the commune of *Toulouse* moves from class 5 to class 4 (Figure 9(c)). The TC method reveals transitions, with three communes now having IRIS units with very high vulnerability, while *Seilh* and *Gagnac-sur-Garonne* remain stable across the three methods.

https://doi.org/10.48088/ejg.t.lag.15.3.154.176

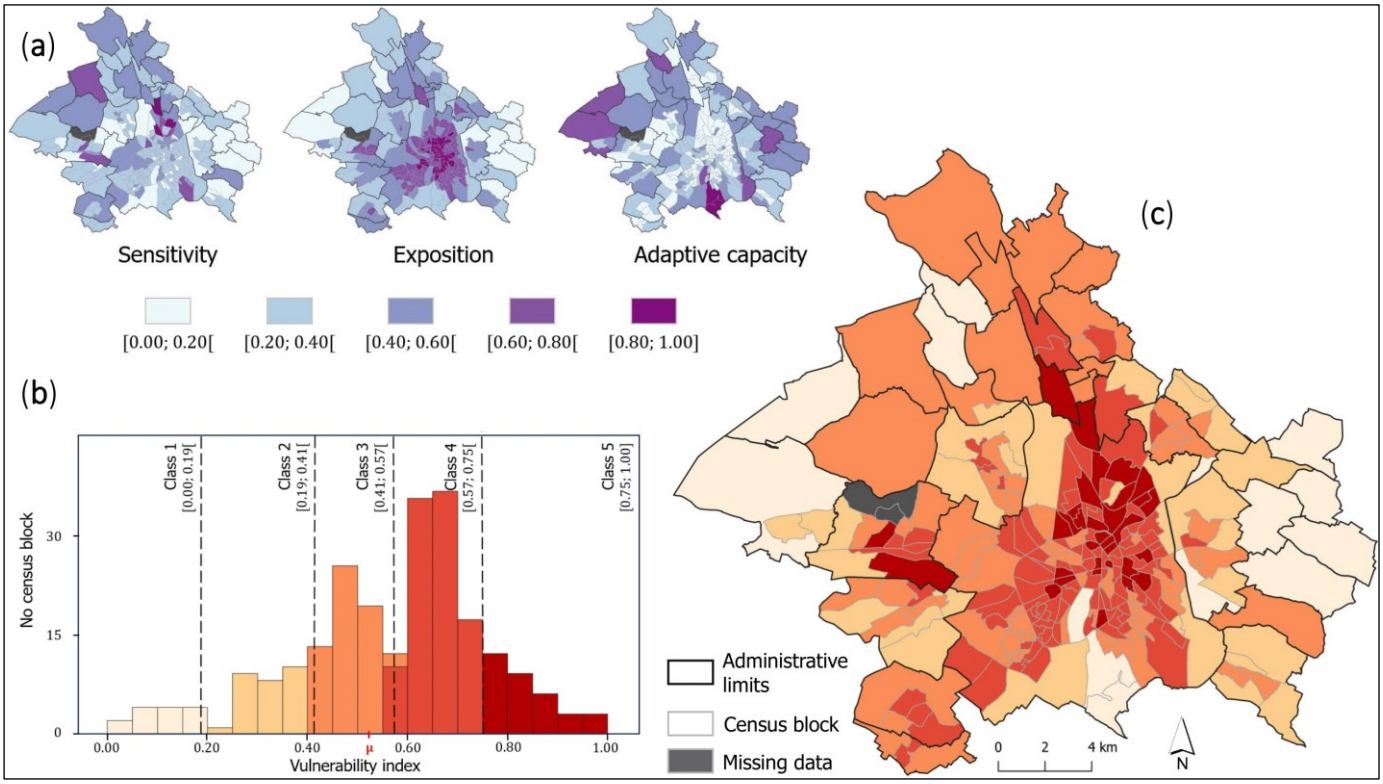

Figure 9. HVI obtained using the theoretical component (TC) method on the Toulouse Métropole. (**a**) Spatial distribution of the three vulnerability factors; (**b**) discretization and statistical distribution of the HVI; (**c**) final HVI.

3.2. Comparison of results

The discrepancies highlighted in earlier sections are explored here in two phases. Initially, we scrutinize the divergence in the vulnerability index classes across IRIS units. Subsequently, we verify whether the spatial distribution patterns of the HVI vary according to the chosen method.

3.2.1. Comparison of IRIS vulnerability classes

To facilitate comparisons in Figure 10(b), the HVI values were discretized into five equal-interval classes (Figure 10(a)). Rather than assessing differences based solely on exact HVI values, which is overly restrictive, discrepancies were identified when the HVIs fell into different classes.

Of the 14 IRIS units initially classified in class 1, denoting the lowest vulnerability, 50% are consistently classified by all three methods, with 43% matching between two methods. This trend extends to class 2, where 51% of IRIS units exhibit agreement across all methods. Consistency is observed both in outlying municipalities to the east and west, such as *Beaupuy* and *Pibrac*, as well as in the first urban ring of Toulouse, including neighborhoods in the municipalities of *Tournefeuille* and *Blagnac* (e.g., *La Ramée* and *Aéroport*). Classes 3 and 4 maintain similar overall proportions, although their numbers are greater, and consequently so are the vulnerability stakes. In detail, ~50% of class 3 census blocks and 40% assigned to class 4 match in all three methods. However, this distribution also suggests that uncertainty persists for a significant number of IRIS units: 72 of the 143 IRIS units in class 3, as well as 72 of the 120 IRIS units in class 4, are inconsistent across the methods. The highest vulnerability class, class 5, follows the same pattern, with similar assessments for ten of the downtown and suburban neighborhoods (e.g., *Ravelin* and *Concorde*), as well as those located in the northeast of Toulouse (*Borderouge Nord*, *Lalande Nord*, and *La Salade*). However, 14 neighborhoods, notably *Cabirol-Ramassiers* in the commune of *Colomiers*, show HVI results in different classes.

Irrespective of the correspondence of classes by spatial location, a dissimilarity in the proportions of IRIS units within the moderate- and high-vulnerability classes according to the different methods is to be noted (Table 5). Indeed, although classes 1 and 2 have an approximately shared proportion (~4%), the bulk of the PCA-HAC HVI statistical distribution places most values in class 3 (54%), whereas PCA and TC agree in placing them in classes 4 and 5 (41% and 8%, respectively, for PCA and 40% and 8%, respectively, for TC).

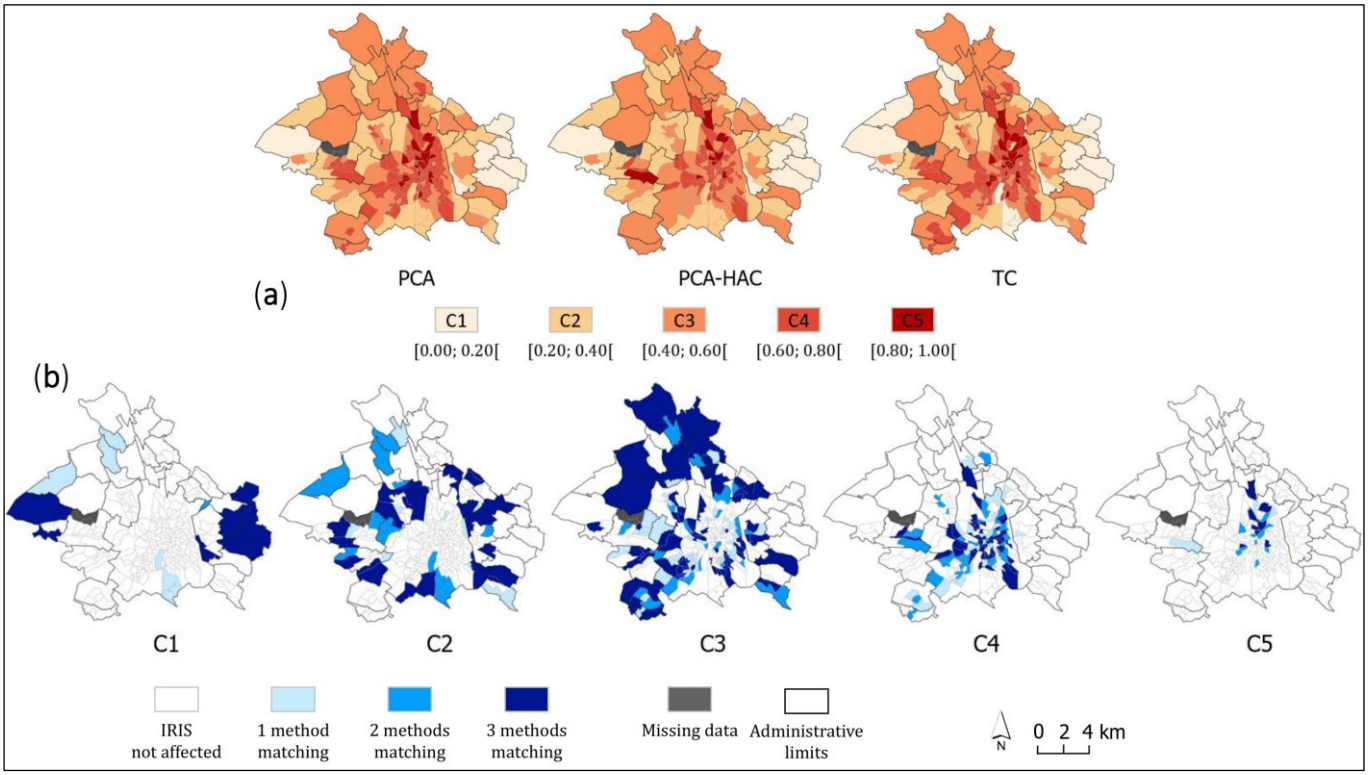

Figure 10. Correspondence of HVI classes according to the method used. (**a**) Final HVI commonly discretized into equal intervals; (**b**) number of times the methods classify the same IRIS unit into the same class displayed in panel (**a**).

Table 5. Number of census blocks (IRIS units) included in the five vulnerability classes.

Method/Class	PCA	PCA-HAC	TC
C1	7	8	14
C2	33	37	28
C3	89	134	86
C4	101	61	100
C5	19	9	21

3.2.2. Comparison of spatial vulnerability patterns

The observations confirm the spatial triptych identified in Section 3.1. As shown in Figure 11, vulnerability progressively decreases with distance from the Toulouse city center/suburbs, extending to the first urban ring and finally the outlying municipalities.

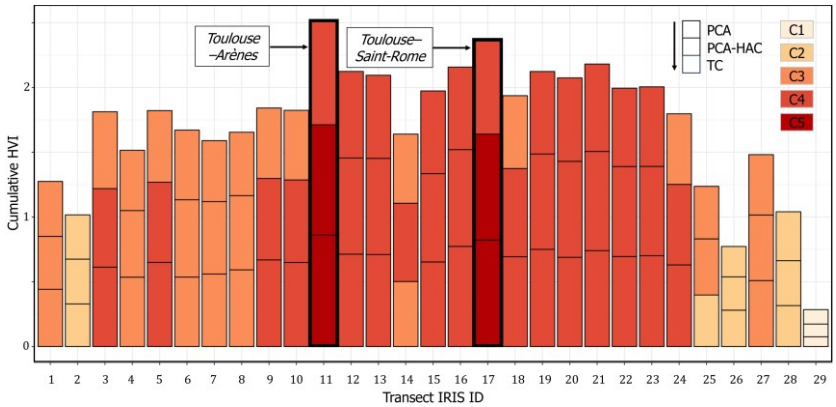

Figure 11. HVI results for the three methodologies for the 29 IRIS units covered by the transect in Figure 2. The vulnerability classes in the legend refer to the discretization in Figure 10. The two IRIS units highlighted with bold lines have the highest transect vulnerabilities. Other IRIS names are provided in Table A2.

The delimitations of this spatial scheme were confirmed and refined using the method presented in Section 2.4, as recommended by Karanja & Kiage (2022), to circumscribe the spatial variability of the HVI scores, via vulnerability hotspots and/or coldspots, and more broadly to reference spatial activities (Panagiotopoulos & Kaliampakos, 2024).

The results reveal two main spatial clusters (Figure 12).

1. Within the *Toulouse* commune limits, numerous highly vulnerable IRIS units are concentrated, delineating two discernible spatial zones. The first encompasses the city center and surrounding suburbs, predominantly situated on the left bank of the Garonne River, stretching northward and eastward. This zone's northern extent is demarcated by IRIS units such as *Fondeyre* and *Bordeouge Sud-Est*, classified as Low-High by PCA and PCA-HAC, and *Sébastopol* for TC, designated as High-High by the other two methodologies. A smaller zone on the right bank exhibits varying boundaries depending on the method applied, including neighborhoods such as *Cartoucherie*, *Hippodrome*, La Grave, and Roguet with PCA and PCA-HAC, and solely Roguet and École Normale with TC.
2. In outlying areas and the first urban ring, two clusters of IRIS units with low vulnerability (Low-Low) prominently emerge, one to the west and the other to the east. The western cluster features communes such as *Pibrac*, *Cornebarrieu*, and *Colomiers* as core constituents, although there are variations in the composition of this cluster. For example, *Mondonville* is referenced solely under the PCA method, while *Fenouillet* and *Aussonne* are classified as Low-Low (PCA) and High-Low (PCA-HAC), respectively. The eastern cluster follows analogous patterns, albeit extending more extensively in the TC method, reaching the southwest of Toulouse. Some municipalities at the cluster periphery also witness shifts in classification based on the methodology employed. Notably, *Quint-Fonsegrives* is categorized as High-Low in PCA-HAC (confirming the prior discussion in Section 3.1.2) and the *Malbou* IRIS in *L'Union* is labeled High-Low in TC.

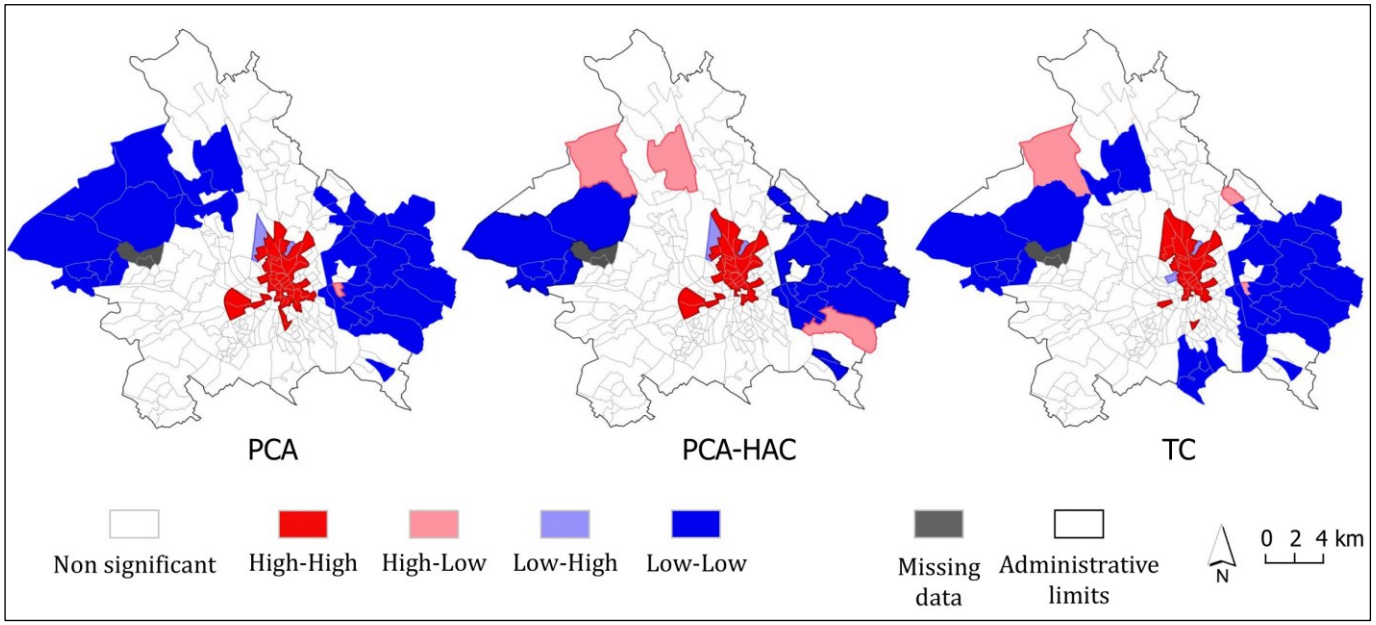

Figure 12. Spatial clusters trained with Anselin–Moran's local spatial statistic I.

While the proportions of IRIS units allocated to vulnerability classes may fluctuate across methodologies, this divergence does not translate into variations in the magnitudes of the vulnerability hotspots but rather in their constituent elements because they encompass equivalent numbers of IRIS units (Table 6). Specifically, of the 259 IRIS units analyzed, 12%, 16%, and 11% are categorized as High-High for PCA, PCA-HAC, and TC, respectively. Likewise, the Low-Low cluster comprises 12% in PCA, 9% in PCA-HAC, and 11% in TC.

Table 6. Percentage of IRIS units included in spatial clusters (trained with Anselin–Moran's local spatial statistic I).

Cluster/Method	High-High	High-Low	Low-High	Low-Low	Non-Significant
PCA	16	0.4	0.8	11	71.8
PCA-HAC	12	1	0.8	9	77.2
TC	12	1	0.8	11	75.2

4. Discussion

The results help explain the spatial and statistical variabilities documented in Section 3, in addition to providing a perspective on a number of limitations that are directly inherent to the various indexing methods, as well as to the input dataset and the spatial reference units that are frequently associated with them.

First, the limitations relate to the "statistical implementation" of the methods, that is, the limitations associated with the statistical modalities required by the methods themselves. This is because the similarities and particularities of the three HVIs are mainly due to the pre-treatment stages and the methodologies themselves. While the HVIs share similarities because of their reliance on similar preprocessing techniques and datasets, their differences emerge in how their vulnerability groups are constructed. PCA often results in unbalanced groups, particularly when dealing with many heterogeneous variables because it seeks linear combinations across all variables while ensuring orthogonality. Consequently, the variance explained decreases after the first dimension, leading to vulnerability groups of varying size and internal consistency as one moves away from the initial groups. In such cases, certain variables may exhibit weak correlations with their respective groups despite preprocessing efforts to the contrary. This weak correlation can result in the dilution of the statistical distribution of these variables among others that are distinct a priori. This statistical limitation, also highlighted by Guo et al. (2019), is especially accentuated in studies of vulnerability to heat because of the variables usually used, which tend to over-represent the socio-economic category relative to other categories. In fact, most of the variables in this group are generally well accounted for in the first components because of the relative similarity of their information, which leads to the remaining, less numerous variables ending up in more composite dimensions. The PCA-HAC method partially addresses this issue via a synthetic variable that is created exclusively for each vulnerability group (Saracco et al., 2018). These groups can then be correlated with each other, ensuring a more specific and sequenced consideration of the various pieces of information to be summarized, although there is always a risk that they will be inexplicable from a theoretical standpoint. Only the TC method makes conceptual sense of the constitution of these factors. However, because these groups are formed without considering the modalities of the dataset, unbalanced results can also be obtained. Here, for example, the Adaptive Capacity group is composed of a single variable, while the Exposure group is mostly made up of variables whose spatial distributions contradict each other, in the same way as for Factor 1 in the PCA method. Furthermore, the "manual" assignment of variables to vulnerability parameters remains entirely subjective and does not facilitate the emergence of common perspectives from one study to another. For example, while Kastendeuch et al. (2023) place income level in the Adaptive Capacity parameter, this study places it in the Sensitivity parameter. Ultimately, it remains unclear "whether theoretical or statistical relationships should determine vulnerability indicators" (Karanja & Kiaga, 2021, p. 5).

Second, beyond explaining the variability, it is also necessary to consider the representation and representativeness of the results obtained. These issues can focus on the input data and spatial reference scales required for the application of indexing approaches, which only locate and evaluate the vulnerability statically. This is because the data in this study for Metropolitan France were derived from a census conducted through an annual survey covering all municipalities over a five-year period (Choffel & Heroguer, 2009) and, therefore, can only partially track demographic changes. As in most other Western countries, socio-demographic data only cover the resident population. Therefore, they do not account for certain daily (or even nightly) activities that occur outside the place of residence, such as professional or leisure activities. Furthermore, they are spatialized into geographical units such as census blocks, whose size and area vary to ensure the anonymity of the surveyed individuals and allow free access to the data. As Karanja & Kiage (2022) point out, this spatial non-uniformity of blocks creates scale and density effects (the MAUP effect). In practice, many IRIS units correspond to entire municipalities, while others cover only neighborhoods, which tends to smooth out internal disparities within these IRIS municipalities. For example, *Cornebarrieu* is often considered a moderately vulnerable municipality; however, it contains a social housing area that would likely have been classified as vulnerable if treated as a separate IRIS unit.

Third, in light of the two previous limitations, the presented dichotomous spatial configuration of city center/periphery must be approached with caution. More broadly, HVIs raise conceptual issues concerning their evaluation, interpretation, and especially their operational implementation. In other words, what information can be gleaned from an HVI assessment and/or what insight into vulnerability can such an assessment actually provide? As observed, the use of three different methodologies reveals that a significant number of IRIS units belong to different vulnerability classes, where an index analysis alone does not allow us to target with certainty a large proportion of areas assessed as vulnerable and even less to understand how and why these areas are vulnerable. Furthermore, the perception of these areas is largely influenced by the evaluators themselves, depending on the data, methodologies, spatial scale, method of scaling the scores, and the choice of classification intervals on the map. Furthermore, this quantification system, through indices/scores, assumes that all vulnerabilities can be captured, compared, and therefore ranked. However, it has been shown that the data usually used cannot comprehensively represent all types of populations and the diversity of their lived experiences (Molina et al., 2023). Lastly, no threshold effect or empirical evidence has yet been demonstrated to measure potential degrees of vulnerability, not even in studies where the HVI is validated by epidemiological data because these studies measure vulnerability only through morbidity and/or mortality (neglecting any other type of vulnerability that is expressed in other ways) and generally focus only on a spatiotemporal scale too narrow to be generalizable.

5. Conclusions

This study analyzed the ability of indexing approaches to provide stable and consistent vulnerability results in light of the current theoretical conceptualization, considering reservations that had already been expressed (Guo et al., 2019) or, more simply, variabilities that had already been revealed (Liu et al., 2020; Zhu et al., 2014) without being relayed and reflected in subsequent studies. For this analysis, we replicated commonly used conditions in this field of research for evaluating vulnerability in the form of an index, considering the same input datasets, the same reference spatial scales, and the same processing methodologies. Accordingly, three methodologies commonly found in the literature were tested to assess the vulnerability of the Toulouse Métropole area on the scale of French national demographic census blocks (IRIS units).

Section 3.1 presented three main spatial patterns common to all three methodologies. These echo the ring-shaped spatial distribution observed by Guo et al. (2019) and Liu et al. (2020), as well as that recorded in other French territories, such as the city of Amiens (Qureshi & Rachid, 2022), the metropolis of Strasbourg (Kastendeuch et al., 2023), and the metropolis of Montpellier (Técher et al., 2023). However, note that these trends are not found in the metropolis of Lyon (Alonso & Renard, 2020), although this needs to be put into perspective because no climatic exposure variable was considered in the Lyon study. For the Toulouse Métropole, given the three HVIs, it is possible to demonstrate the following:

1. census tracts in the city center and suburbs of Toulouse have high vulnerability;
2. municipalities in the first (and sometimes second) ring of Toulouse and the northern metropolitan area have moderate vulnerability; and

3. peripheral municipalities to the west and east of the metropolis have low vulnerability.

These observations were supported and explained by the analysis of the correspondence of the vulnerability classes in Section 3.2.1, which identified eight IRIS units within the municipality of Toulouse as priorities in all three methodologies—*Concorde*, *Ravelin*, *Nègreneys*, *Raynal*, *Camille Pujol*, *La Salade*, *Lalande Nord*, and *Borderouge Nord*—while seven IRIS units around the agglomeration appeared less sensitive to high vulnerability—*Zone d'Activités Sud*, *Beaupuy*, *Flourens*, *Mondouzil*, *Mons*, *Campagne*, and *Pin-Balma*. At the same time, a high percentage of IRIS units were assigned to different vulnerability classes (approximately 40%–60% depending on the vulnerability class), without any demonstrated spatial logic, just as Guo et al. (2019) illustrated with their maps in which downtown census blocks and outlying areas were classified differently depending on the methodology considered. Here, this dissimilarity can be explained in part by the fact that the PCA and TC methods have a majority of IRIS units evenly distributed between moderate- and high-vulnerability classes, unlike the PCA-HAC method, which yielded more moderate results. These assertions were further verified and affirmed in this study because no weighting was applied, meaning that this variability is intrinsically based on the methods themselves rather than their parameterizations.

The analysis in Section 3.2.2 refined and circumscribed the previously identified spatial structures. The findings of Karanja & Kiage (2022) were again verified in this study, i.e., the spatial dynamics of HVIs are diverse from one method to another and highlight the variability of vulnerability hotspots. In more analytical terms, high-vulnerability spatial clusters were notably concentrated on both banks of the Garonne River in the densely populated IRIS units of the downtown area of Toulouse: a first cluster on the right bank with relatively stable boundaries according to the various methodologies and a secondary cluster on the left bank with composition varying by methodology. Similarly, the composition and location of low-vulnerability clusters showed variations, with more municipalities grouped to the west in the PCA method and to the east in the TC method, extending even to the southeast of Toulouse.

Finally, our findings are consistent with previous studies that have explored the variability of HVIs according to various factors such as the spatial unit (Zhang et al., 2018), spatial weighting (Karanja & Kiage, 2022), or, as seen here, the indexing methodology used (Guo et al., 2019). In particular, our study corroborates and further reinforces Guo et al.'s (2019) conclusions, more prominently highlighting variabilities by considering three methods rather than two.

To conclude, studies stipulate that the variability in the results of various HVI methodologies highlight the multiple facets of vulnerability and, as such, should not hinder its application or use (Karanja & Kiage, 2022) because the discussed limitations can be countered by analyzing the vulnerability at a finer spatial scale via advances with respect to the data and processing used (Sun et al., 2022; Zhang et al., 2018). Despite the potential of these methods to resolve certain issues, such as those related to the effects of geostatistical biases, the fundamental conceptual limits intrinsic to what a statistical index is and represents remain invariable. Indeed, the one-dimensional focus of indexing approaches remains antinomic with current theoretical paradigms that recognize vulnerability as a complex, multi-dimensional system. At the outset, the input data can indeed be used to list the various vulnerability factors, in line with the theoretical conceptualization. However, these factors always end up in a hierarchy, both in their representation (only the most related variables are ultimately represented) and in their intensity, even though there is no justification for this process, as explained in Section 4. In this respect, the interpretation of the results is misleading because an HVI ultimately provides only part of the information concerning vulnerability: the census blocks prioritized by HVI maps are not those containing the most people with characteristics deemed vulnerable but those containing the most people with the most statistically similar characteristics. In the operational translation of the results—which is what an HVI is designed to do—this observation leads us to reconsider the ability of an HVI to function as an autonomous decision-making tool because it could, for the reasons given above, lead to poorly located and/or poorly calibrated adaptation and mitigation measures.

At present, an HVI only offers an initial diagnosis of an area, providing preliminary elements for reflection and analysis. However, such data need to be supplemented by other approaches, particularly qualitative ones, to build a more complete picture of the needs of vulnerable populations. Rather than simply assigning degrees of vulnerability, it would be more coherent to turn to profiling approaches that can precisely identify groups in need of equitable support. While embracing these qualitative methodologies, as some social science studies have already done, it is crucial to retain a practical and spatial dimension to ensure the operationality of the results. In addition, encouraging interdisciplinary collaboration, knowledge exchange, and comparisons of methods is essential to ensure the theory–evaluation–operation *continuum* and ultimately incorporate vulnerability information into urban planning documents.

Within this perspective, the city of Toulouse should continue to develop its vulnerability maps following a potential approach based on the percentage of the population present in different perimeters and changing levels of risk, including other environmental risks (e.g., air quality and noise). At the level of the Toulouse Métropole, ongoing work is being carried out concerning the role of green infrastructure as a heat mitigation measure (Jung et al., 2024; Mackey et al., 2012). Additionally, a second initiative is being developed to identify, provide, and develop a climate shelter network for the population based on the model implemented in Barcelona (Estevez et al., 2024).

Funding: This research project received support from the French Environment and Energy Management Agency (ADEME) under the PACT2e APR pro-gram, contract number 21DAD0080

Acknowledgments: We would like to thank Sylvain Bigot (Professor, IGE-PHYREV) and Sandra Rome (Associate Professor, IGE-HMCIS) for their expertise in this study. We thank Martha Evonuk, PhD, from Evonuk Scientific Editing (http://evonukscientificediting.com) for editing a draft of this manuscript. This article stems from the initial findings and perspectives identified in a previous study (Lagelouze, 2022) conducted within the same research project.

Data Availability Statement: As noted in Table 1, four data sources were used: IGN; MApUCE-UHI; CESBIO-OSO; and Insee.

Conflicts of Interest: The authors declare no conflict of interest.

Appendix A

Table A1. Names of the Toulouse Métropole municipalities according to the IDs displayed in Figure 2.

ID [.]	Municipality
1	*Fonbeauzard*
2	*Beaupuy*
3	*Mons*
4	*Tournefeuille*
5	*Mondonville*
6	*Aucamville*
7	*Seilh*
8	*Castelginest*
9	*Launaguet*
10	*Pin-Balma*
11	*Fenouillet*
12	*Colomiers*
13	*Cornebarrieu*
14	*Balma*
15	*Blagnac*
16	*Montrabé*
17	*Toulouse*
18	*Lespinasse*
19	*L'Union*
20	*Cugnaux*
21	*Villeneuve-Tolosane*
22	*Beauzelle*
23	*Mondouzil*
24	*Gagnac-sur-Garonne*
25	*Saint-Orens-de-Gameville*
26	*Flourens*
27	*Bruguières*
28	*Aussonne*
29	*Quint-Fonsegrives*
30	*Saint-Jean*
31	*Saint-Jory*
32	*Gratentour*
33	*Pibrac*
34	*Saint-Alban*

Appendix B

Table A2. Names of the municipalities and IRIS units in the Toulouse Métropole covered by the transect in Figure 2.

Transect IRIS ID [.]	Municipality name	IRIS ID [.]	IRIS name
1	*Cugnaux*	311570105	*Quartier Périphérique*
2	*Tournefeuille*	315570104	*La Ramée*
3	*Toulouse*	315555503	*Saint-Simon Ouest*
4	*Toulouse*	315555601	*Basso Cambo*
5	*Toulouse*	315555701	*Ferdinand de Lesseps*
6	*Toulouse*	315555401	*Les Vergers*
7	*Toulouse*	315555402	*Antonio Machado*
8	*Toulouse*	315553201	*Morvan*
9	*Toulouse*	315553202	*Loire*
10	*Toulouse*	315553401	*Tellier*
11	*Toulouse*	315553301	*Arènes*
12	*Toulouse*	315551502	*Déodat de Séverac*
13	*Toulouse*	315551501	*Sainte-Lucie*
14	*Toulouse*	315550601	*Teinturiers*
15	*Toulouse*	315550502	*Dalbade*

16	*Toulouse*	315550501	*Filatiers*
17	*Toulouse*	315550102	*Saint-Rome*
18	*Toulouse*	315550302	*Wilson*
19	*Toulouse*	315550301	*Occitane*
20	*Toulouse*	315551102	*Colombette*
21	*Toulouse*	315551103	*Gabriel Péri*
22	*Toulouse*	315552003	*La Gloire*
23	*Toulouse*	315554302	*Heredia*
24	*Toulouse*	315554301	*Louis Plana*
25	*Toulouse*	315554303	*Patinoire de la Fraternité*
26	*Balma*	310440108	*Zone d'Activités Nord*
27	*Balma*	310440104	*Le Château*
28	*Montrabé*	313890000	*Montrabé*
29	*Beaupuy*	310530000	*Beaupuy*

Appendix C

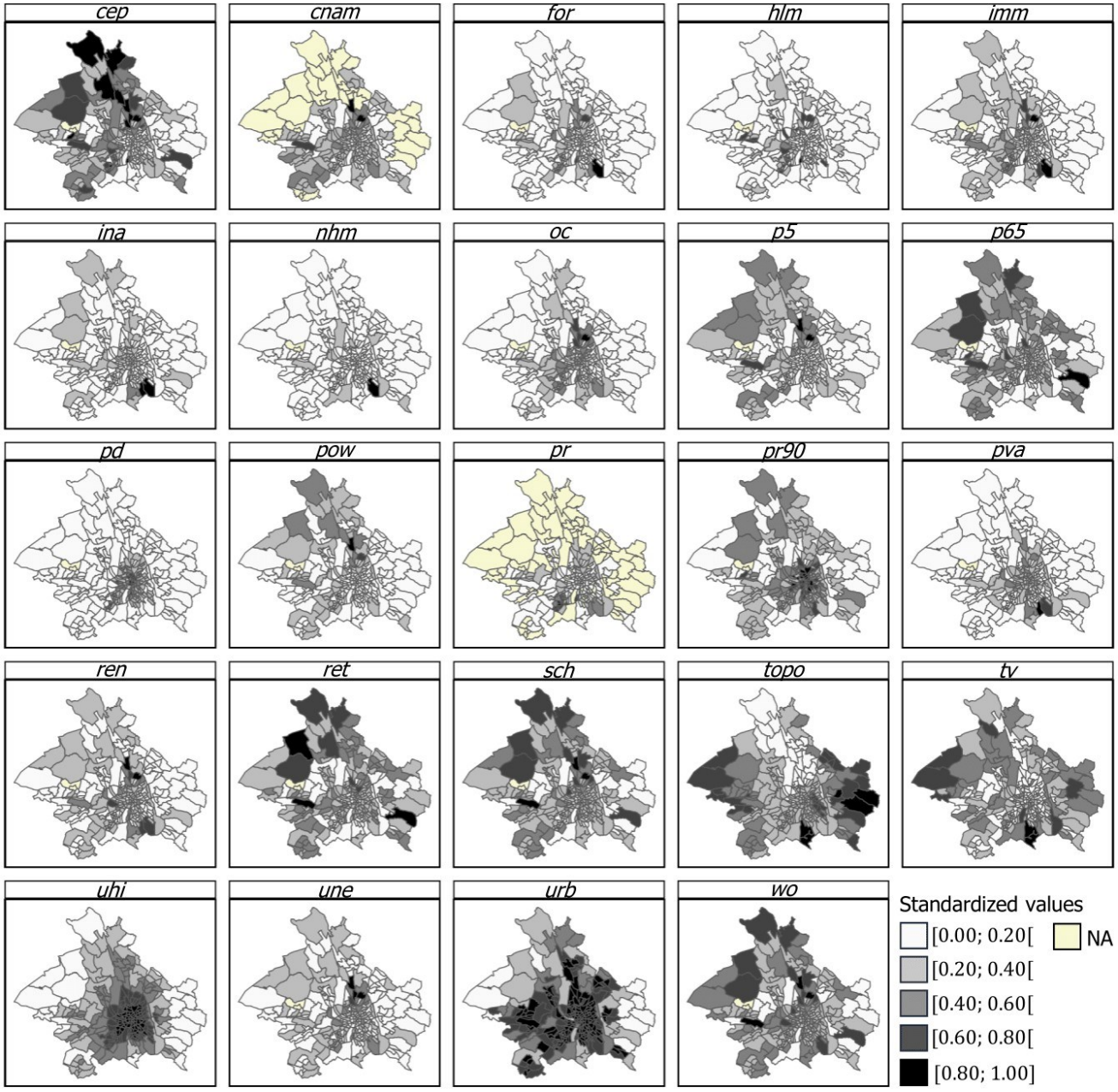

Figure A1. Mapping of the vulnerability variables selected for the construction of the HVIs, with values standardized to 1 using the min-max method.

Appendix D

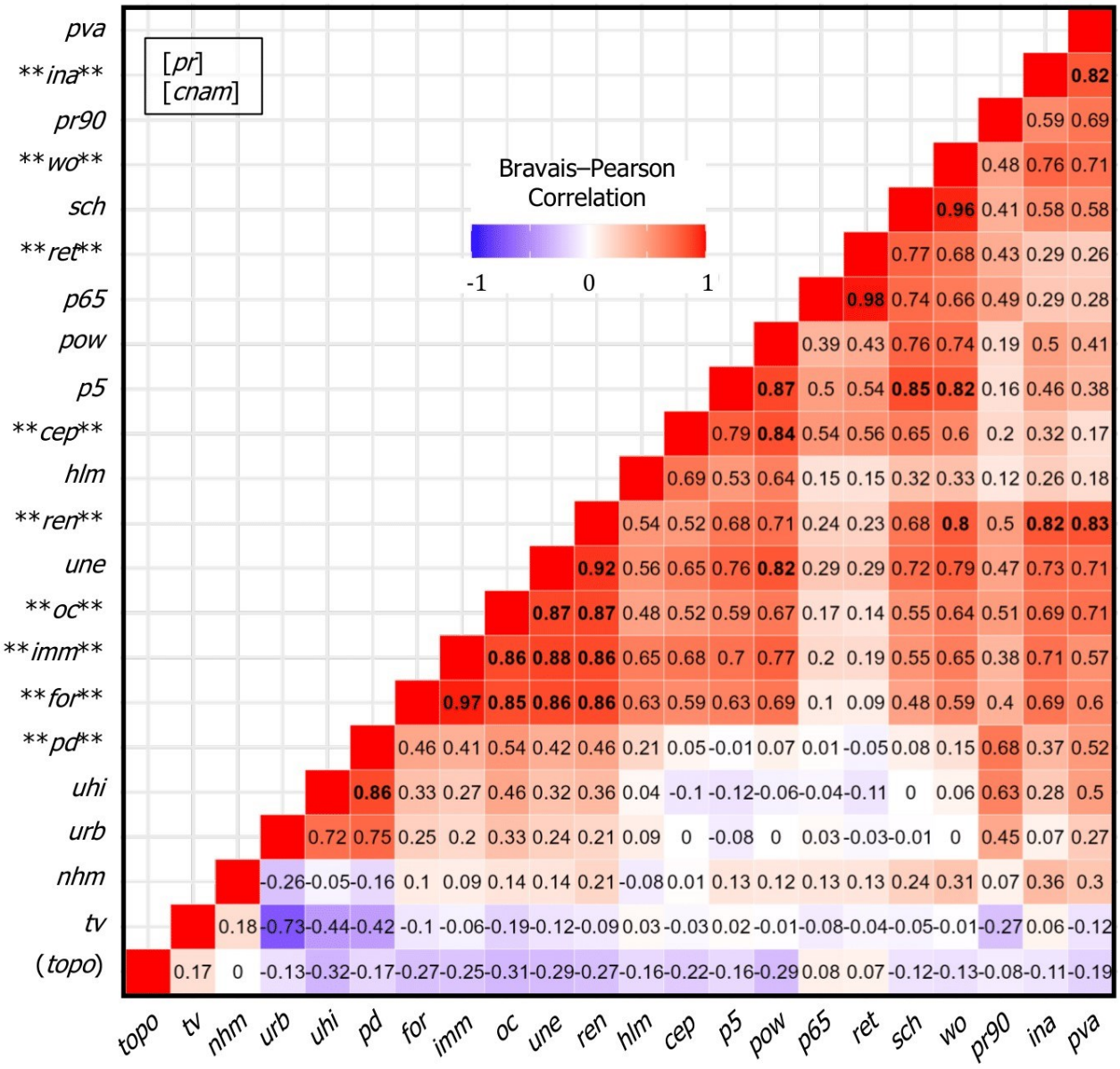

Figure A2. Bravais–Pearson correlation matrix of the vulnerability variables selected for HVI construction. Correlations greater than or equal to 0.8 and less than or equal to −0.8 are in bold. Variables deleted because of missing data are denoted by [variable]. Variables judged collinear are represented as **variable**. Variables suppressed by PCA treatments are indicated as (variable).

References

Alonso, L., & Renard, F. (2020). A Comparative Study of the Physiological and Socio-Economic Vulnerabilities to Heat Waves of the Population of the Metropolis of Lyon (France) in a Climate Change Context. *International Journal of Environmental Research and Public Health*, 17(3), Article 3. https://doi.org/10.3390/ijerph17031004

Anastassakos, I., & d'Aubigny, G. (1984). L'utilisation des tests de sphéricité pour la recherche de la dimension de l'espace latent en analyse factorielle classique et en analyse en composantes principales. *Revue de Statistique Appliquée*, 32(2), 45–57. http://www.numdam.org/item/RSA_1984__32_2_45_0/

Anselin, L. (1995). Local Indicators of Spatial Association—LISA. *Geographical Analysis*, 27(2), 93–115. https://doi.org/10.1111/j.1538-4632.1995.tb00338.x

Ballester, J., Quijal-Zamorano, M., Méndez Turrubiates, R. F., Pegenaute, F., Herrmann, F. R., Robine, J. M., Basagaña, X., Tonne, C., Antó, J. M., & Achebak, H. (2023). Heat-related mortality in Europe during the summer of 2022. *Nature Medicine*, 29(7), Article 7. https://doi.org/10.1038/s41591-023-02419-z

Bao, J., Li, X., & Yu, C. (2015). The Construction and Validation of the Heat Vulnerability Index, a Review. *International Journal of Environmental Research and Public Health*, 12(7), 7220–7234. https://doi.org/10.3390/ijerph120707220-

Becerra, S. (2012). Vulnérabilité, risques et environnement: L'itinéraire chaotique d'un paradigme sociologique contemporain. *VertigO - la revue électronique en sciences de l'environnement*, Volume 12 Numéro 1, Article Volume 12 Numéro 1. https://doi.org/10.4000/vertigo.11988

Benmarhnia, T., Deguen, S., Kaufman, J. S., & Smargiassi, A. (2015). Review Article: Vulnerability to Heat-related Mortality: A Systematic Review, Meta-analysis, and Meta-regression Analysis. *Epidemiology* (Cambridge, Mass.), 26(6), 781–793. https://doi.org/10.1097/EDE.0000000000000375

Benmarhnia, T., Kihal-Talantikite, W., Ragettli, M., & Deguen, S. (2017). Small-area spatiotemporal analysis of heatwave impacts on elderly mortality in Paris: A cluster analysis approach. *Science of the Total Environment*, 592, 288. https://doi.org/10.1016/j.scitotenv.2017.03.102

Berger, J.-L. (2022). Analyse factorielle exploratoire et analyse en composantes principales: Guide pratique. https://doi.org/10.13140/RG.2.2.16206.18246

Blaikie, P., Cannon, T., Davis, I., & Wisner, B. (Eds.). (1994). At risk: Natural hazards, people's vulnerability, and disasters (1. publ). Routledge.

Chavent, M., Kuentz-Simonet, V., Labenne, A., & Saracco, J. (2022). Multivariate Analysis of Mixed Data : The R Package PCAmixdata. https://doi.org/10.48550/arXiv.1411.4911

Chavent, M., Kuentz-Simonet, V., Liquet, B., & Saracco, J. (2012). ClustOfVar: An R Package for the Clustering of Variables. *Journal of Statistical Software*, 50, 1–16. https://doi.org/10.18637/jss.v050.i13

Choffel, P., & Heroguer, P. (2009). Population, démographie [SIG Ville]. Système d'Information Géographique de la politique de la Ville. https://sig.ville.gouv.fr/page/48

Climate Copernicus. (2023). 2022 saw record temperatures in Europe and across the world. Climate Copernicus. https://climate.copernicus.eu/2022-saw-record-temperatures-europe-and-across-world

Cronbach, L. J. (1951). Coefficient alpha and the internal structure of tests. *Psychometrika*, 16(3), 297–334. https://doi.org/10.1007/BF02310555

Cutter, S. (1996). Societal Vulnerability to Environmental Hazards. *Progress in Human Geography*, 20, 529–539. https://doi.org/10.1177/030913259602000407

Cutter, S. L., Boruff, B. J., & Shirley, W. L. (2003). Social Vulnerability to Environmental Hazards. *Social Science Quarterly*, 84(2), 242–261. https://doi.org/10.1111/1540-6237.8402002

d'Ercole, R. (1998). Approches de la vulnérabilité et perspectives pour une meilleure logique de réduction des risques. Pangea infos, 29/30, 20.

de Sherbinin, A., Bukvic, A., Rohat, G., Gall, M., McCusker, B., Preston, B., Apotsos, A., Fish, C., Kienberger, S., Muhonda, P., Wilhelmi, O., Macharia, D., Shubert, W., Sliuzas, R., Tomaszewski, B., & Zhang, S. (2019). Climate vulnerability mapping: A systematic review and future prospects. *WIREs Climate Change*, 10(5), e600. https://doi.org/10.1002/wcc.600

Dousset, B., Gourmelon, F., Giraudet, E., Laaidi, K., Zeghnoun, A., Bretin, P., & Vandentorren, S. (2011). Evolution climatique et canicule en milieu urbain: Apport de la télédétection à l'anticipation et à la gestion de l'impact sanitaire (p. 77). https://hal.archives-ouvertes.fr/hal-00620833

Dubreuil, V. (2022). Le changement climatique en France illustré par la classification de Köppen. *La Météorologie*, 116, Article 116. https://doi.org/10.37053/lameteorologie-2022-0012

Ebi, K. L., Capon, A., Berry, P., Broderick, C., Dear, R. de, Havenith, G., Honda, Y., Kovats, R. S., Ma, W., Malik, A., Morris, N. B., Nybo, L., Seneviratne, S. I., Vanos, J., & Jay, O. (2021). Hot weather and heat extremes: Health risks. *The Lancet*, 398(10301), 698–708. https://doi.org/10.1016/S0140-6736(21)01208-3

Ebi, K. L., Vanos, J., Baldwin, J. W., Bell, J. E., Hondula, D. M., Errett, N. A., Hayes, K., Reid, C. E., Saha, S., Spector, J., & Berry, P. (2021). Extreme Weather and Climate Change: Population Health and Health System Implications. *Annual Review of Public Health*, 42(1), 293–315. https://doi.org/10.1146/annurev-publhealth-012420-105026

Estevez B., Hidalgo J. and Bonhomme M. (2024). Anticipatory action and future living in a context of increasing temperatures: an analysis from the Barcelona Climate Shelter Network. Book chapter for Cities as Anticipatory Systems, Springer. Manuscript submitted for publication.

Forceville, G., Lemonsu, A., Goria, S., Stempfelet, M., Host, S., Alessandrini, J.-M., Cordeau, E., & Pascal, M. (2024). Spatial contrasts and temporal changes in fine-scale heat exposure and vulnerability in the Paris region. *Science of The Total Environment*, 906, 167476. https://doi.org/10.1016/j.scitotenv.2023.167476

Guo, X., Huang, G., Jia, P., & Wu, J. (2019). Estimating Fine-Scale Heat Vulnerability in Beijing Through Two Approaches: Spatial Patterns, Similarities, and Divergence. *Remote Sensing*, 11(20), Article 20. https://doi.org/10.3390/rs11202358

Huang, G., Zhou, W., & Cadenasso, M. L. (2011). Is everyone hot in the city? Spatial pattern of land surface temperatures, land cover and neighborhood socioeconomic characteristics in Baltimore, MD. *Journal of Environmental Management*, 92(7), 1753–1759. https://doi.org/10.1016/j.jenvman.2011.02.006

Inostroza, L., Palme, M., & de la Barrera, F. (2016). A Heat Vulnerability Index: Spatial Patterns of Exposure, Sensitivity and Adaptive Capacity for Santiago de Chile. *PloS One*, 11(9), e0162464. https://doi.org/10.1371/journal.pone.0162464

Insee. (2024). Découpage infracommunal | Insee [Institutionnel]. Institut national de la statistique et des études économiques (INSEE). https://www.insee.fr/fr/information/2017499

Insee. (2024). Dossier complet – Intercommunalité-Métropole de Toulouse Métropole (243100518) | Insee [Institutionnel]. Institut national de la statistique et des études économiques (INSEE). https://www.insee.fr/fr/statistiques/2011101?geo=EPCI-243100518#chiffre-cle-1

Inserm. (2004). Surmortalité liée à la canicule d'août 2003 (p. 76). https://www.inserm.fr/wp-content/uploads/2017-11/inserm-rapportthematique-surmortalitecaniculeaout2003-rapportfinal.pdf

IPCC. (2021). Climate Change 2021 - The Physical Science Basis: Working Group I Contribution to the Sixth Assessment Report of the Intergovernmental Panel on Climate Change (1re éd.). Cambridge University Press. https://doi:10.1017/9781009157896

IPCC. (2023). Climate Change 2022 - Impacts, Adaptation and Vulnerability: Working Group II Contribution to the Sixth Assessment Report of the Intergovernmental Panel on Climate Change (1re éd.). Cambridge University Press. https://doi:10.1017/9781009325844

Jung, M. C., Yost, M. G., Dannenberg, A. L., Dyson, K., & Alberti, M. (2024). Legacies of redlining lead to unequal cooling effects of urban tree canopy. *Landscape and Urban Planning*, 246(105028). https://doi.org/10.1016/j.landurbplan.2024.105028

Kaiser, H. F. (1958). The varimax criterion for analytic rotation in factor analysis. *Psychometrika*, 23(3), 187–200. https://doi.org/10.1007/BF02289233

Kaiser, H. F. (1974). An index of factorial simplicity. *Psychometrika*, 39(1), 31–36. https://doi.org/10.1007/BF02291575

Karanja, J., & Kiage, L. (2021). Perspectives on spatial representation of urban heat vulnerability. *Science of The Total Environment*, 774, 145634. https://doi.org/10.1016/j.scitotenv.2021.145634

Karanja, J., & Kiage, L. (2022). Scale implications and evolution of a social vulnerability index in Atlanta, Georgia, USA. *Natural Hazards*, 113(1), 789–812. https://doi.org/10.1007/s11069-022-05324-9

Kastendeuch, P., Massing, N., Schott, E., Philipps, N., & Lecomte, K. (2023). Vulnérabilité et îlot de chaleur urbain: Les facteurs du risque thermique nocturne à Strasbourg. *Climatologie*, 20, 9. https://doi.org/10.1051/climat/202320009

Laaidi, K., Zeghnoun, A., Dousset, B., Bretin, P., Vandentorren, S., Giraudet, E., & Beaudeau, P. (2012). The Impact of Heat Islands on Mortality in Paris during the August 2003 Heat Wave. *Environmental Health Perspectives*, 120(2), 254–259. https://doi.org/10.1289/ehp.1103532

Lagelouze, T. (2022). Comparaison de méthodes d'évaluation statistiques de la vulnérabilité sociale à la hausse de la chaleur en milieu urbain : application aux métropoles de Toulouse, Grenoble, Lyon et Paris. Master 2 Mention « GAED » Parcours: GEOgraphie Information Interface Durabilité EnvironnementS. Université Grenoble Alpes, 69 p. https://dumas.ccsd.cnrs.fr/dumas-03774994 ;

Lemarque, M. (2023, août 26). Toulouse. 2003 ou 2023 : Quelle canicule a été la plus sévère selon Météo France ? actu.fr. https://actu.fr/occitanie/toulouse_31555/toulouse-2003-ou-2023-quelle-canicule-a-ete-la-plus-severe-selon-meteo-france_60000605.html

Lemonsu, A., Viguié, V., Daniel, M., & Masson, V. (2015). Vulnerability to heat waves: Impact of urban expansion scenarios on urban heat island and heat stress in Paris (France). *Urban Climate*, 14, 586–605. https://doi.org/10.1016/j.uclim.2015.10.007

Li, D., & Bou-Zeid, E. (2013). Synergistic Interactions between Urban Heat Islands and Heat Waves: The Impact in Cities Is Larger than the Sum of Its Parts. *Journal of Applied Meteorology and Climatology*, 52(9), 2051–2064. https://doi.org/10.1175/JAMC-D-13-02.1

Li, F., Yigitcanlar, T., Nepal, M., Thanh, K. N., & Dur, F. (2022). Understanding Urban Heat Vulnerability Assessment Methods: A PRISMA Review. *Energies*, 15(19), Article 19. https://doi.org/10.3390/en15196998

Liu, X., Yue, W., Yang, X., Hu, K., Zhang, W., & Huang, M. (2020). Mapping Urban Heat Vulnerability of Extreme Heat in Hangzhou via Comparing Two Approaches. *Complexity*, e9717658. https://doi.org/10.1155/2020/9717658

Mackey, C. W., Lee, X., & Smith, R. B. (2012). Remotely sensing the cooling effects of city scale efforts to reduce urban heat island. *Building and Environment*, 49, 348-358. https://doi.org/10.1016/j.buildenv.2011.08.004

Meehl, G. A., & Tebaldi, C. (2004). More intense, more frequent, and longer lasting heat waves in the 21st century. *Science (New York, N.Y.)*, 305(5686), 994–997. https://doi.org/10.1126/science.1098704

Molina, G., Hureau, L., & Lamberts, C. (2023). Les citadins face aux fortes chaleurs: Vulnérabilités, vécus habitants, santé et adaptations. Rapport du programme de recherche CNRS - IRSTV - Nantes Métropole " Habitants des villes et climat ." https://hal.science/hal-04172893

Naughton, M. P., Henderson, A., Mirabelli, M. C., Kaiser, R., Wilhelm, J. L., Kieszak, S. M., Rubin, C. H., & McGeehin, M. A. (2002). Heat-related mortality during a 1999 heat wave in Chicago. *American Journal of Preventive Medicine*, 22(4), 221–227. https://doi.org/10.1016/s0749-3797(02)00421-x

Nayak, S. G., Shrestha, S., Kinney, P. L., Ross, Z., Sheridan, S. C., Pantea, C. I., Hsu, W. H., Muscatiello, N., & Hwang, S. A. (2018). Development of a heat vulnerability index for New York State. *Public Health*, 161, 127–137. https://doi.org/10.1016/j.puhe.2017.09.006

OECD, European Union, & Joint Research Centre - European Commission. (2008). Handbook on Constructing Composite Indicators: Methodology and User Guide. OECD. https://doi.org/10.1787/9789264043466-en

Oke, T. R. (1973). City size and the urban heat island. *Atmospheric Environment* (1967), 7(8), 769–779. https://doi.org/10.1016/0004-6981(73)90140-6

Oke, T. R. (1978). Boundary Layer Climates. Routledge.

Peres-Neto, P., Jackson, D., & Somers, K. (2005). How Many Principal Components? Stopping Rules for Determining the Number of Non-Trivial Axes Revisited. *Computational Statistics & Data Analysis*, 49, 974–997. https://doi.org/10.1016/j.csda.2004.06.015

Panagiotopoulos, G., & Kaliampakos, D. (2024). Accessibility, Rural Depopulation & the Modified Areal Unit Problem: An Analysis of Mainland Greece. *European Journal of Geography*, 15(1), Article 1. https://doi.org/10.48088/ejg.g.pan.15.1.042.053

Pigeon, P. (2002). Réflexions sur les notions et les méthodes en géographie des risques dits naturels. *Annales de géographie*, 111(627), 452–470. https://doi.org/10.3406/geo.2002.21624

Quenault, B. (2015). La vulnérabilité, un concept central de l'analyse des risques urbains en lien avec le changement climatique. *Les Annales de la Recherche Urbaine*, 110(1), 138–151. https://doi.org/10.3406/aru.2015.3175

Qureshi, A. M., & Rachid, A. (2022). Heat Vulnerability Index Mapping: A Case Study of a Medium-Sized City (Amiens). *Climate*, 10(8), Article 8. https://doi.org/10.3390/cli10080113

Rakotomalala, R. (2012). Stratégies de détermination du nombre d'axes en ACP (Analyse en Composantes Principales). https://eric.univ-lyon2.fr/ricco/tanagra/fichiers/fr_Tanagra_Nb_Components_PCA.pdf

Rand, W. M. (1971). Objective Criteria for the Evaluation of Clustering Methods. *Journal of the American Statistical Association*, 66(336), 846–850. https://doi.org/10.1080/01621459.1971.10482356

Reghezza-Zitt, M. (2023). Sociétés humaines et territoires dans un climat qui change. Du réchauffement climatique global aux politiques climatiques (ISSN : 2492-7775) [Document]. Géoconfluences; École normale supérieure de Lyon. https://geoconfluences.ens-lyon.fr/informations-scientifiques/dossiers-thematiques/changement-global/articles-scientifiques/rechauffement-climatique-politiques-climatiques

Robine, J.-M., Cheung, S. L. K., Le Roy, S., Van Oyen, H., Griffiths, C., Michel, J.-P., & Herrmann, F. R. (2008). Death toll exceeded 70,000 in Europe during the summer of 2003. Comptes Rendus Biologies, 331(2), 171–178. https://doi.org/10.1016/j.crvi.2007.12.001

Sanders, L. (1989). L'analyse des données appliquée à la géographie. Groupement d'intérêt public RECLUS.

Saracco, J., Chavent, M., Audin-Garcia, L., Lespinet-Najib, V., & Ron-Angevin, R. (2018). Classification de variables et analyse multivariée de données mixtes issues d'une étude BCI. *Ingénierie Cognitique*, 2(1). https://doi.org/10.21494/ISTE.OP.2018.0311

Semenza, J. C., Rubin, C. H., Falter, K. H., Selanikio, J. D., Flanders, W. D., Ho.we, H. L., & Wilhelm, J. L. (1996). Heat-Related Deaths during the July 1995 Heat Wave in Chicago. *New England Journal of Medicine*, 335(2), 84–90. https://doi.org/10.1056/NEJM199607113350203

Soomar, S. M., & Soomar, S. M. (2023). Identifying factors to develop and validate a heat vulnerability tool for Pakistan – A review. *Clinical Epidemiology and Global Health*, 19, 101214. https://doi.org/10.1016/j.cegh.2023.101214

Suher-Carthy, M., Lagelouze, T., Hidalgo, J., Schoetter, R., Touati, N., Jougla, R., & Masson, V. (2023). Urban heat island intensity maps and local weather types description for a 45 French urban agglomerations dataset obtained from atmopsheric numerical simulations. *Data in Brief*, 50, 109437. https://doi.org/10.1016/j.dib.2023.109437

Suher-Carthy, M. (2021). Translation of Urban Climate Analysis Output Using Chorematic Representation: Case of French Cities. *Theseus*, 80. https://urn.fi/URN:NBN:fi:amk-2021110119105

Sun, Y., Li, Y., Ma, R., Gao, C., & Wu, Y. (2022). Mapping urban socio-economic vulnerability related to heat risk : A grid-based assessment framework by combing the geospatial big data. *Urban Climate*, 43, 101169. https://doi.org/10.1016/j.uclim.2022.101169

Técher, M., Ait Haddou, H., & Aguejdad, R. (2023). Urban Heat Island's Vulnerability Assessment by Integrating Urban Planning Policies: A Case Study of Montpellier Méditerranée Metropolitan Area, France. *Sustainability*, 15(3), Article 3. https://doi.org/10.3390/su15031820

Theys, J., & Fabiani, J.-L. (1987). La Société vulnérable: Évaluer et maîtriser les risques. Presses de l'École normale supérieure.

Thomas, K., Hardy, R. D., Lazrus, H., Mendez, M., Orlove, B., Rivera-Collazo, I., Roberts, J. T., Rockman, M., Warner, B. P., & Winthrop, R. (2019). Explaining differential vulnerability to climate change: A social science review. Wiley Interdisciplinary Reviews. *Climate Change*, 10(2), e565. https://doi.org/10.1002/wcc.565

Tuccillo, J. V., & Spielman, S. E. (2022). A Method for Measuring Coupled Individual and Social Vulnerability to Environmental Hazards. *Annals of the American Association of Geographers*, 112(6), 1702–1725. https://doi.org/10.1080/24694452.2021.1989283

Wolf, T., Chuang, W.-C., & McGregor, G. (2015). On the Science-Policy Bridge: Do Spatial Heat Vulnerability Assessment Studies Influence Policy? *International Journal of Environmental Research and Public Health*, 12(10), Article 10. https://doi.org/10.3390/ijerph121013321

Wolf, T., McGregor, G., & Analitis, A. (2013). Performance Assessment of a Heat Wave Vulnerability Index for Greater London, United Kingdom. *Weather, Climate, and Society*, 6(1), 32–46. https://doi.org/10.1175/WCAS-D-13-00014.1

World Meteorological Organization. (2021). WMO Atlas of Mortality and Economic Losses from Weather, Climate and Water Extremes (1970–2019) (p. 90). https://library.wmo.int/viewer/57564/download?file=1267_Atlas_of_Mortality_en.pdf&type=pdf&navigator=1

Xu, Z., Sheffield, P. E., Su, H., Wang, X., Bi, Y., & Tong, S. (2014). The impact of heat waves on children's health: A systematic review. *International Journal of Biometeorology*, 58(2), 239–247. https://doi.org/10.1007/s00484-013-0655-x

Yeo, I., & Johnson, R. A. (2000). A new family of power transformations to improve normality or symmetry. *Biometrika*, 87(4), 954–959. https://doi.org/10.1093/biomet/87.4.954

Yin, S., Ren, C., Zhang, X., Hidalgo, J., Schoetter, R., Kwok, Y. T., & Lau, K. K.-L. (2022). Potential of Synthetizing Climatopes and Local Climate Zones for Urban Climatic Planning Recommendations: A Case Study in Toulouse, France. *Cybergeo: Revue Européenne de Géographie / European Journal of Geography*. https://doi.org/10.4000/cybergeo.39417

Zhang, W., McManus, P., & Duncan, E. (2018). A Raster-Based Subdividing Indicator to Map Urban Heat Vulnerability: A Case Study in Sydney, Australia. *International Journal of Environmental Research and Public Health*, 15(11), 2516. https://doi.org/10.3390/ijerph15112516

Zhu, Q., Liu, T., Lin, H., Xiao, J., Luo, Y., Zeng, W., Zeng, S., Wei, Y., Chu, C., Baum, S., Du, Y., & Ma, W. (2014). The spatial distribution of health vulnerability to heat waves in Guangdong Province, China. *Global Health Action*, 7. https://doi.org/10.3402/gha.v7.25051

https://doi.org/10.48088/ejg.t.lag.15.3.154.176